AD-A093 053 MARK RESOURCES INC MARINA DEL REY CA F/G 17/9
RFSS. VOLUME 2. EXTENDED TARGET MODEL: REAL-TIME SIMULATION PRO--ETC(U)
DEC 78 R L MITCHELL DAAK40-78-C-0031
UNCLASSIFIED MRI-149-39 NL

1 OF 1
AD A
093053

END
DATE
FILMED
1-81
DTIC

AD A093053

LEVEL III

U.S. ARMY MIRADCOM

RFSS. Volume 2.

EXTENDED TARGET MODEL: REAL-TIME SIMULATION PROGRAM.
(VOL 2 OF FINAL TECHNICAL REPORT)

TECH NOTE 105-052

29 DEC 78

MRI-149-39, MRI-TN-105-052

Final technical rept.,

PREPARED FOR: RF SYSTEMS BRANCH (DRDMI-TDR)
SYSTEMS SIMULATION DIRECTORATE
TECHNOLOGY LABORATORY
US ARMY MIRADCOM
REDSTONE ARSENAL, AL 35809

DAAK40-78-C-0031

PREPARED BY: DR. R. L. MITCHELL
MARK RESOURCES, INC.
4676 ADMIRALTY WAY
SUITE 303
MARINA DEL REY, CA 90291

391 766

MARK RESOURCES INCORPORATED

EXTENDED TARGET MODEL: REAL-TIME SIMULATION PROGRAM

MRI REPORT 149-39

R. L. MITCHELL

29 DECEMBER 1978

Volume 2 of a Final Technical Report under
Contract DAAK40-78-C-0031

Under the Sponsorship of:

U.S. Army Missile R&D Command (DRDMI-TDR)
Redstone Arsenal, AL 35809

Accession For
NTIS GRA&I
DDC TAB
Unannounced
Justification
See AD for
By TN 105-029
Distribution/
Availability Codes
Dist | Avail and/or special
A

(all intentionally blank as next page starts new section.)

4676 ADMIRALTY WAY / SUITE 303 / MARINA DEL REY, CALIFORNIA 90291 / (213) 822-4955

FOREWORD

The work performed under Contract DAAK40-78-C-0031 that resulted in specific deliverables (principally computer programs) is described in two volumes of a final report. This is Volume 2, which describes the work that led to the extended target model. Volume 1, entitled "Distributed Clutter Model: Real-Time FFT Program," describes the work relevant to that subject.

The AP120B array processor programs described in this report (but documented elsewhere) were designed and developed by Dr. I. P. Bottlik, as well as the interfaces to the host computer and Digital Signal Generator. Dr. Bottlik was assisted by Mr. D. L. Brandon.

TABLE OF CONTENTS

LIST OF FIGURES

LIST OF TABLES

1. INTRODUCTION AND SUMMARY

This report describes a real-time simulation procedure for generating replicas of an extended target signal to be radiated from the RFSS array to a missile system radar under test. The procedure is purely deterministic. It is based on identifying in the model the location and amplitude of the predominant scattering centers on the target; during the real-time simulation, rays are traced to each scatterer so that the radiated signal is the phasor superposition of the component rays. The missile and target geometries are modeled with six degrees of freedom, and the target motions of roll, pitch, and yaw are included. The instantaneous target aspect is determined so that any scattering dependencies on target aspect can be included in the model. The range dimension of the target is sorted into range bins corresponding to taps on a tapped-delay line. For each tap an angular glint centroid is computed.

The procedure permits any target to be simulated; the scattering centers on the target must be identified beforehand as part of the model. This information forms the data base from which the signal is generated. Listings of a Fortran program are included in Appendix B. As written, the program will not run in real time. It is assumed that some portion of it will be implemented on an AP120B array processor to satisfy the real-time requirement.

2. THE MEDIUM-RANGE TARGET MODEL

Three types of extended target models were discussed in Reference 1, the short-, medium-, and long-range models. The long-range model has only limited application in the RFSS, and the short-range model, which is based on radiating signals into specific angles on the receive beam, requires accurate knowledge of the receive antenna boresight axis position. Because of these disadvantages it was decided to concentrate on the medium-range model, which assumes that one is always working in the linear portion of the monopulse receive beam. The target model is uncoupled from the receive antenna position as long as this assumption is valid. In this section we derive the form of the modulation signals for the medium-range model.

2.1 The Scintillating Target

For the moment, let us assume that the target is composed of a number of point scatterers at the same effective range (no range extent compared to the resolution cell, but the scatterers may differ in range by many wavelengths). If σ_k denotes the radar cross section (RCS) of the k^{th} scatterer as viewed from a particular target aspect, then we can assign a complex quantity to the k^{th} scatterer, V_k, where $|V_k|^2 = \sigma_k$ and the phase accounts for the slightly different range (measured in wavelengths) among the scatterers (or differences in the reflection properties). If all scatterers are illuminated with the same transmit and receive gain we can replace the set of scatterers by a single scatterer with the effective complex reflection coefficient given by

$$V_e = \sum_k V_k \qquad (1)$$

The phasor summation in (1) accounts for the target signal scintillation as measured by the radar. With the exception of a scale factor to account for the radar range equation, it is the modulation function that is applied to the delayed transmitted waveform to simulate the target.

2-Blank

2.2 The Glint Centroid

Let us take the same target model above and assume that the receiver is a monopulse system so that it is capable of measuring an angle to the target. We will again assume that the target has no range extent. If all scatterers are illuminated by the same transmit antenna gain, and all are within the linear region of the receive monopulse beam, the radar will measure an angle to the target that is effectively the electrical centroid given for the one-dimensional case by

$$\hat{\theta} = \theta_o + \mathrm{Re}\left\{\frac{\sum\limits_k (\theta_k - \theta_o) V_k}{\sum\limits_k V_k}\right\} \tag{2}$$

where θ_o is a reference angle and θ_k is the angle associated with the k^{th} scatterer.

Equation (2) is insensitive to the angle of the receive antenna boresight axis. It is valid as long as all scatterers are within the linear region of the monopulse beam (i.e., the target model will be uncoupled from the radar antenna). In practice, this linear region extends approximately only to about the half-power beamwidth of the sum-channel beam. In Appendix A we derive the maximum angular extent of the target for which the above assumptions are valid, and it is given roughly by the half-power beamwidth (one-way).

2.3 Range Extent

Modern radars usually have high range resolution so that the target may extend over several range resolution cells (this is the definition of a range-extended target). In this case only a few of the scatterers on a target will fall within any given range cell. The response in a range cell is given by a slightly modified from of (1) and (2) as

$$V_e = \sum_k \omega_k V_k \tag{3}$$

$$\hat{\theta} = \theta_o + \mathrm{Re}\left\{\frac{\sum_k (\theta_i - \theta_o)\omega_k V_k}{\sum \omega_k V_k}\right\} \tag{4}$$

where ω_k accounts for the variable range gate weighting of the k^{th} scatterer in the range cell of interest. It is a function of only the differential delay between the k^{th} scatterer and the center of the range gate (see Section 4).

In general, a strict application of (3) and (4) requires that the range gate timing be known in the receiver. However, as was derived in Reference 1 it is possible to accurately simulate the range extent of the target when the timing is unknown by the use of a resampling technique based upon a tapped-delay line implementation. The taps must be spaced no further apart than 50% of the range resolution cell size. The technique consists simply of applying (3) and (4) to each tap of the tapped-delay line. The weights ω_k are thus defined as the tap weights, and they are a function of the differential delay between the location of the scatterer and the tap. For a spacing of 50% of the range resolution cell (the most efficient spacing) only four taps will receive any significant contribution from each scatterer (see Section 4).

2.4 Implementing the Medium-Range Model on the RFSS

The use of (3) and (4) creates a sequence of effective complex voltage samples $V_e(n)$ and glint centroids $\hat{\theta}(n)$ as a function of range as is sketched in Figure 1. In order to simulate the composite signal we have to create a

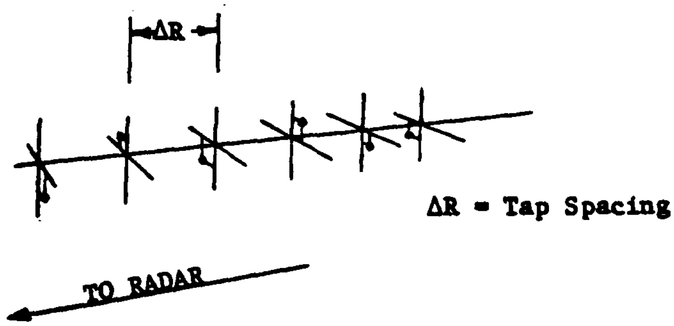

Figure 1. Physical Arrangement of Resampled Scatterers for Range-Extended Target

different glint angle for each tap on a tapped-delay line. One approach would be to utilize a separate RFSS signal generation channel for each tap, but the approach would be limited to four taps because there are only four RFSS channels. A far better approach would be to utilize the supertriad devised by Mott [2], which we now discuss.

To simulate a point target in the RFSS, signals are directed to three horns on the array (a triad) and with proper amplitude and phase control on each horn the point target can be made to appear anywhere within the triad. For our purposes we will not restrict the three sources to coincide with the ABC triad configuration of the RFSS array. We will use separate RFSS channels to generate each signal so that the three points of radiation can be placed anywhere on the RFSS array. We will designate this configuration as a "supertriad." The elements of the supertriad can be spaced further apart than the horn spacing in the conventional ABC triad.

For a range-extended target we will build upon the supertriad with a tapped-delay line as shown in Figure 2. The RFSS signal channels are designated A, B, and C in the figure to coincide with the elements of the supertriad. The A, B, and C channel signals will each be radiated from fixed points on the array, regardless of the delay (until the engagement geometry is updated); however, by controlling the modulation signals (A1, A2, ..., A8, B1, B2, ..., C8 in Figure 2) the phase center can be made to appear anywhere within the supertriad (and slightly outside it) at each tap on the tapped-delay line. Thus we have the situation that is sketched in Figure 3. Note that the location of the phase center in angle at each tap can be chosen independently of the other taps.

2.5 The Modulation Signals at the Taps

Equations (3) and (4) define the signal amplitude, phase, and angle (there will be two angles involved) corresponding to one tap of the tapped-delay line. To compute the modulation signal that is applied to the supertriad, let us refer to Figure 4 where we place the origin of the x,y coordinate system at the centroid of the supertriad composed of equal sides. In other words, Point A is located at the coordinate $(0, d/\sqrt{3})$, Point B at

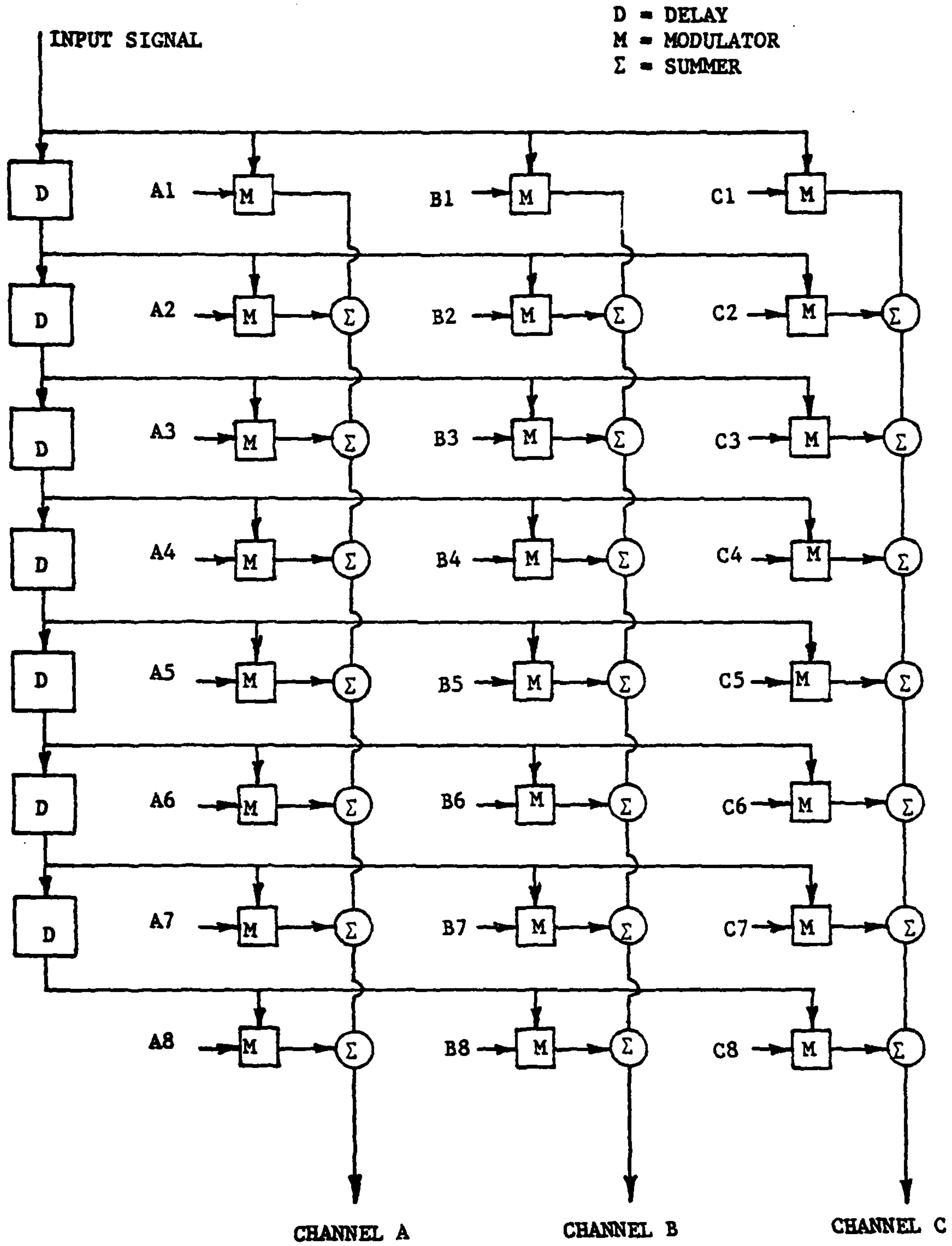

Figure 2. Supertriad Configuration with Delay Line

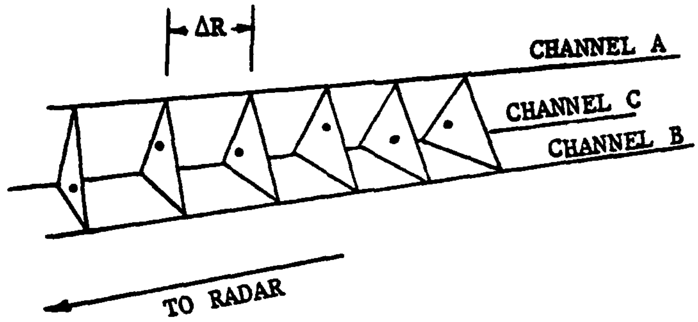

Figure 3. Simulating Extended Target with Supertriad and Tapped-Delay Line

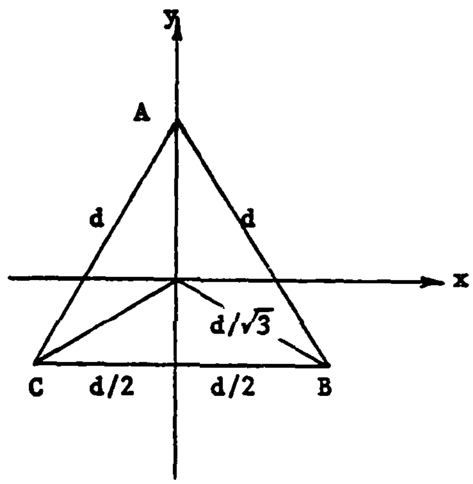

Figure 4. Geometry of Supertriad

$(d/2, -d/2\sqrt{3})$, and Point C at $(-d/2, -d/2\sqrt{3})$, where d is the spacing of the points. Let's define θ to be in the x-direction so that

$$x = D(\hat{\theta} - \theta_o) \tag{5}$$

where $\hat{\theta}$ is given by (4) and D is the distance between the radar under test and the RFSS array. With a similar equation to (4) we will define ϕ to be in the y-direction so that

$$y = D(\hat{\phi} - \phi_o) \tag{6}$$

The reference angles (θ_o, ϕ_o) coincide with the origin of the x,y coordinates. The modulation signals that are applied to the elements of the supertriad are now

$$V_A = V_e \left(\frac{1}{3} + \frac{2}{\sqrt{3}} \frac{y}{d}\right) \tag{7}$$

$$V_B = V_e \left(\frac{1}{3} + \frac{x}{d} - \frac{1}{\sqrt{3}} \frac{y}{d}\right) \tag{8}$$

$$V_C = V_e \left(\frac{1}{3} - \frac{x}{d} - \frac{1}{\sqrt{3}} \frac{y}{d}\right) \tag{9}$$

The above computations must be applied to each tap.

2.6 Choosing the Size of the Supertriad

In general, the size of the supertriad should be chosen to encompass the angular extent of the target. At long range we can choose d small so the accuracy will be best (but d should not be less than the RFSS horn spacing). As the target range decreases we must increase d accordingly. As long as the elements of the supertriad are within the linear region of the monopulse beam, there will be no error due to the fact that we are radiating from three points simultaneously, instead of a single one at the desired phase center. However, we will eventually reach a limiting value of d where we are no longer within the linear region of the monopulse beam.

To determine this limit let us approximate the one-dimensional response to the monopulse system by

$$\hat{\theta} = \theta(1 - \alpha\theta^2) \tag{10}$$

where θ is the angle of a point scatterer measured from the boresight axis. Let us place two horns spaced by $\Delta = d/D$ as in Figure 5 with one at an angle θ_o from the origin, and we will place a point scatterer at the origin. From the left horn we will radiate a signal with a relative amplitude θ/Δ and from the right horn a signal of relative amplitude $(1 - \theta/\Delta)$. The composite response of the monopulse system is the sum of the individual responses as

$$\begin{aligned}\hat{\theta} &= \theta(1-\alpha\theta^2)(1-\theta/\Delta) + (\theta-\Delta)[1-\alpha(\theta-\Delta)^2]\,(\theta/\Delta) \\ &= \alpha\theta(\Delta-\theta)(\Delta-2\theta) \qquad (11)\end{aligned}$$

The angle would be zero if the system were linear (i.e., $\alpha = 0$), so (11) represents the error in simulating a scatterer on the boresight axis with two horns configured as in Figure 5. A local maximum (extremum) of (11) occurs at $\theta = \Delta(1/2 \pm 1/\sqrt{12})$ and is given by

$$\hat{\theta}_{ext} = \frac{1}{3\sqrt{12}}\,\alpha\Delta^3 \qquad (12)$$

A typical value for α is $1.70/\theta^2_{3dB}$, where θ_{3dB} is the one-way half-power beamwidth of the monopulse sum channel. For this case and $\theta_{3dB} = 12°$ we have plotted the error given by (11) in Figure 6. The abscissa is $\theta - \Delta/2$, so that a value of $\theta - \Delta/2 = 0$ corresponds to the two horns being placed symmetrically about the origin. The curves are also symmetrical about the origin in Figure 6. For $\alpha = 1.70/\theta^2_{3dB}$ we can rewrite (12) as

$$\frac{\hat{\theta}_{ext}}{\theta_{3dB}} = .164\left(\frac{\Delta}{\theta_{3dB}}\right)^2 \qquad (13)$$

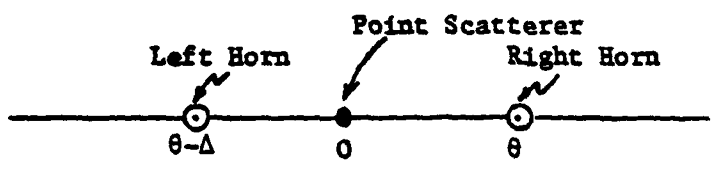

Figure 5. Simulating Point Scatterer with Two Horns

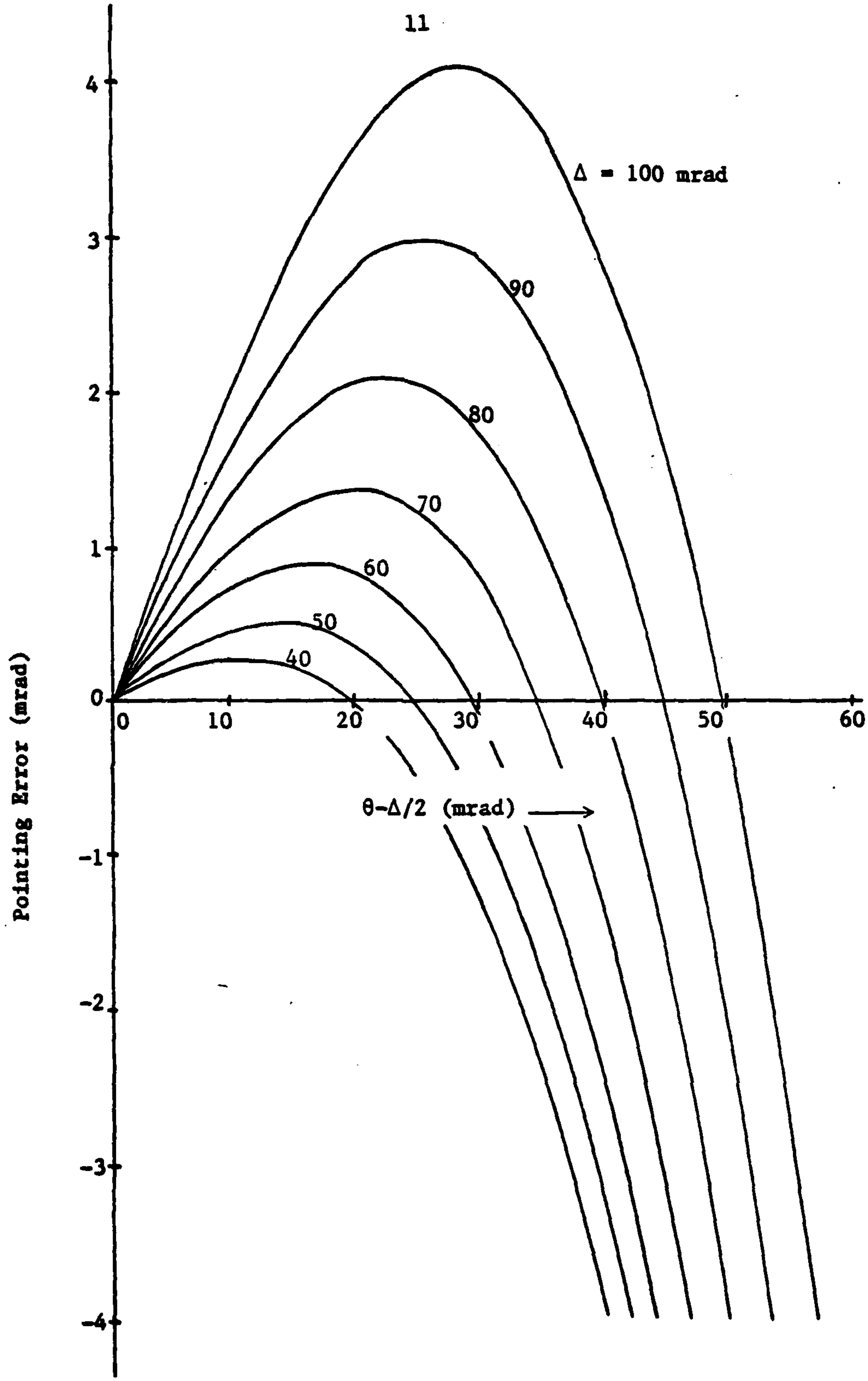

Figure 6. Pointing Error for Two-Horn Case

This Page Intentionally Left Blank

3. ENGAGEMENT GEOMETRY AND COORDINATE TRANSFORMS

In this section we define the quantities that are required to specify the engagement geometry and the transformations used to obtain the ray coordinates of each scatterer in the missile coordinate system.

3.1 Specification of Target Position and Dynamics

At a given instant of time the target c.g. is characterized by a location (x_o, y_o, z_o) and rate ($\dot{x}_o$, $\dot{y}_o$, $\dot{z}_o$) in an inertial coordinate system referenced to the ground. The x-y plane is parallel to the ground and the z-axis is positive *downward*.

The target coordinate system is sketched in Figure 7 and is defined such that the x-axis is the longitudinal axis of the aircraft target, positive in the direction of the nose; the y-axis is in the direction of the right wing; and the z-axis is down. The origin of the target coordinate system is at the target c.g.

The orientation of the target is given by a series of three consecutive coordinate system rotations, the order of which is important. First, the target is oriented so that its x,y,z axes are parallel to the ground-referenced x,y,z axes. Then the following rotations (clockwise, looking out from the coordinate origin) are applied:

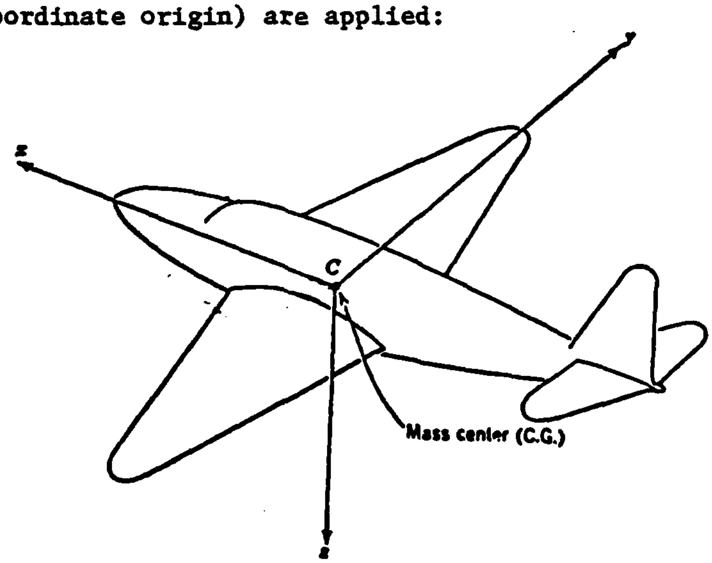

Figure 7. Definition of Target Coordinate System

1. a rotation Ψ about the z-axis
2. a rotation Θ about the y-axis
3. a rotation Φ about the x-axis

The target is undergoing roll, pitch, and yaw motion in its own coordinate system. We define P,Q,R to be the roll, pitch, and yaw body rotation rates (clockwise looking out from the coordinate origin) as sketched in Figure 8. The relationship of P,Q,R to the angles Ψ,Θ,Φ is

$$\dot{\Theta} = Q \cos \Phi - R \sin \Phi \tag{14}$$

$$\dot{\Phi} = P + (Q \sin \Phi + R \cos \Phi) \tan \Theta \tag{15}$$

$$\dot{\Psi} = (Q \sin \Phi + R \cos \Phi) \sec \Theta \tag{16}$$

In general, the excursion of these motions will be over small angles.

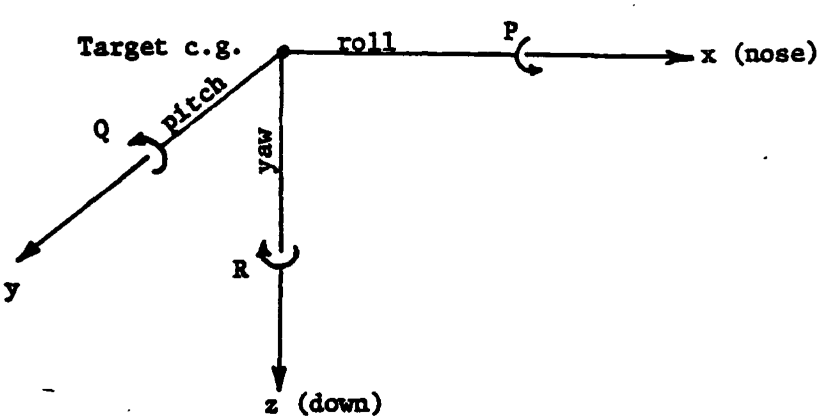

Figure 8. Roll, Pitch, and Yaw Motions

3.2 Specification of Missile Position and Dynamics

A the same instant of time for which the target dynamics are defined, we define the location of the missile as (x_m,y_m,z_m) and the velocity as $(\dot{x}_m,\dot{y}_m,\dot{z}_m)$, where the coordinate system is the same ground-referenced system used for the target.

3.3 Specification of Target Scatterers

The target aspect is defined in Figure 9, where the azimuth and elevation angles of the radar (as viewed from the target) are α and β, respectively. The aspect angle from the x- or roll-axis, which we designate as γ, is given by

$$\cos\gamma = \cos\alpha\cos\beta \tag{17}$$

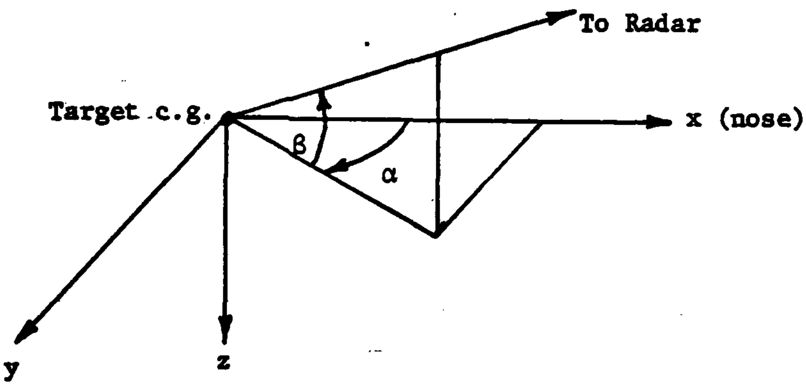

Figure 9. Target Aspect

At a particular target aspect, a set of scattering centers will be specified in terms of the location (x_k, y_k, z_k) and amplitude (A_k) of each scatterer, where the subscript k designates the scatterer number and amplitude is defined as the square root of radar cross section (RCS). In general, A_k, x_k, y_k, z_k will all be functions of the target aspect. A specification of this functional relationship is the target model.

3.4 The ABC Vectors

Let us define three mutually perpendicular unit vectors, the origin of which is at the target c.g. Vector A points to the missile radar, Vector B is in the horizontal plane pointing to the left as viewed from the missile, and Vector C completes the definition of a right-hand system (it points downward as viewed from the missile). In terms of the conventional radar

coordinates (referenced to the ground), $\bar{A}$ points in the direction of decreasing range, $\bar{B}$ in the negative azimuth direction, and $\bar{C}$ in the negative elevation direction. In terms of the RFSS array, $\bar{A}$ points from the target c.g. on the RFSS array to the missile radar, $\bar{B}$ points left as viewed from the missile, and $\bar{C}$ points down.

From the previous definitions we have the direction cosines of $\bar{A}$ in the ground referenced coordinate system given by

$$a_x = (x_m - x_o)/r_o \tag{18}$$

$$a_y = (y_m - y_o)/r_o \tag{19}$$

$$a_z = (z_m - z_o)/r_o \tag{20}$$

where r_o is the range to the target c.g. given by

$$r_o^2 = (x_m - x_o)^2 + (y_m - y_o)^2 + (z_m - z_o)^2 \tag{21}$$

Let us define

$$\rho^2 = (x_m - x_o)^2 + (y_m - y_o)^2 \tag{22}$$

so that we can write the direction cosines of the $\bar{B}$ and $\bar{C}$ vectors as

$$b_x = -(y_m - y_o)/\rho \tag{23}$$

$$b_y = (x_m - x_o)/\rho \tag{24}$$

$$b_z = 0 \tag{25}$$

$$c_x = -b_y(z_m - z_o) \tag{26}$$

$$c_y = b_x(z_m - z_o) \tag{27}$$

$$c_z = \rho \tag{28}$$

Note that $\bar{C} = \bar{A} \times \bar{B}$.

3.5 Transformation of a Vector to Target Coordinates

Given an arbitrary vector $\bar{A}$ in the ground-referenced coordinate system, we can define it in the target coordinate system by three successive coordinate rotations. First, if we rotate the z-axis by Ψ (clockwise looking out) we obtain the direction cosines in the new system

$$u_x = a_x \cos \Psi + a_y \sin \Psi \tag{29}$$

$$u_y = -a_x \sin \Psi + a_y \cos \Psi \tag{30}$$

$$u_z = a_z \tag{31}$$

Next, let us rotate the y-axis by Θ (clockwise looking out) so that

$$v_x = u_x \cos \Theta - u_z \sin \Theta \tag{32}$$

$$v_y = u_y \tag{33}$$

$$v_z = u_x \sin \Theta + u_z \cos \Theta \tag{34}$$

Finally, we will rotate the x-axis by Φ (clockwise looking out) to obtain

$$w_x = V_x \tag{35}$$

$$w_y = V_y \cos \Phi + V_z \sin \Phi \tag{36}$$

$$w_z = -V_y \sin \Phi + V_z \cos \Phi \tag{37}$$

Since several vectors will be transformed in this manner we will designate the resulting vector in the target coordinate system as $W(\bar{A})$, where the original vector was $\bar{A}$. The direction cosines of $W(\bar{A})$ are designated as $w_x(\bar{A})$, $w_y(\bar{A})$, and $w_z(\bar{A})$.

The A,B, and C vectors (defined in Section 3.4) in the target coordinate system are thus $W(\bar{A})$, $W(\bar{B})$, and $W(\bar{C})$. Note that $W(\bar{C}) = W(\bar{A}) \times W(\bar{B})$, so that after transforming the first two vectors we could find the third by

$$w_x(\bar{C}) = w_y(\bar{A})w_z(\bar{B}) - w_z(\bar{A})w_y(\bar{B}) \tag{38}$$

$$w_y(\bar{C}) = w_z(\bar{A})w_x(\bar{B}) - w_x(\bar{A})w_z(\bar{B}) \tag{39}$$

$$w_z(\bar{C}) = w_x(\bar{A})w_y(\bar{B}) - w_y(\bar{A})w_x(\bar{B}) \tag{40}$$

3.6 Target Aspect Angle

Let us refer to Figure 9 where $W(\bar{A})$ is the vector pointing to the radar. The azimuth angle α is given by

$$\tan \alpha = w_y(\bar{A})/w_x(\bar{A}) \tag{41}$$

and the elevation angle β by

$$\sin \beta = -w_z(\overline{A}) \tag{42}$$

(remember that $W(\overline{A})$ is a unit vector). The aspect angle measured from the roll axis, γ, is given by

$$\cos \gamma = \cos \alpha \cdot \cos \beta = w_x(\overline{A}) \tag{43}$$

3.7 Projection of Scatterers onto ABC Vectors

Given a scattering center located at (x_k, y_k, z_k) in target coordinates, the projection of this coordinate onto the A,B,C-vectors is simply the dot product onto each vector. Thus we will write

$$\Delta a_k = x_k w_x(\overline{A}) + y_k w_y(\overline{A}) + z_k w_z(\overline{A}) \tag{44}$$

$$\Delta b_k = x_k w_x(\overline{B}) + y_k w_y(\overline{B}) + z_k w_z(\overline{B}) \tag{45}$$

$$\Delta c_k = x_k w_x(\overline{C}) + y_k w_y(\overline{C}) + z_k w_z(\overline{C}) \tag{46}$$

where we are interpreting the scatterer location to be an increment applied to the target c.g. While the distance from the radar to the scatterer is based on the sum of the vectors from the radar to the target c.g. and the target c.g. to the scatterer, we can considerably simplify matters by assuming that the latter vector is small in comparison with the first (such an assumption is consistent with the medium-range target model). Thus the range to the scatterer is essentially $r_o - \Delta a_k$; thus the differential range is defined by

$$\Delta r_k = -\Delta a_k \tag{47}$$

Viewed from the radar the azimuth and elevation angles (measured from the target c.g.) are $-\Delta b_k / r_o$ and $-\Delta c_k / r_o$, respectively, where positive angles are defined right and up.

3.8 Scatterer Motion

We will assume that the yaw, pitch, and roll motion of the target is confined to small angles. With this assumption the target motion (excluding

translational motion of the target c.g.) will not affect the location of the scattering center as far as the ability of the radar to resolve or measure it. We do not have to take this motion into account when computing the location of the scattering center.

However, the radar is sensitive to motion of the scattering center. For small angles, the motion of the scattering center in the target coordinate system is given by

$$\dot{x}_k = z_k Q - y_k R \tag{48}$$

$$\dot{y}_k = x_k R - z_k P \tag{49}$$

$$\dot{z}_k = y_k P - x_k Q \tag{50}$$

where P,Q, and R are the roll, pitch, and yaw body rates defined in Section 3.1. The differential range rate of the scatterer induced by target motion is given by the derivative of (44) as

$$\Delta\dot{r}_k = -\Delta\dot{a}_k = -[\dot{x}_k w_x(\bar{A}) + \dot{y}_k w_y(\bar{A}) + \dot{z}_k w_z(\bar{A})] \tag{51}$$

This quantity is to be added to the range rate of the target c.g., which is the derivative of (21) as

$$\dot{r}_o = [(x_m - x_o)(\dot{x}_m - \dot{x}_o) + (y_m - y_o)(\dot{y}_m - \dot{y}_o) + (z_m - z_o)(\dot{z}_m - \dot{z}_o)]/r_o \tag{52}$$

3.9 Effective Radiated Power for the RFSS

The problem is to simulate a target on the RFSS array so that the power received by the missile radar under test will be equivalent to what would be received by the actual target. From the radar range equation for a reference point scatterer we can write

$$P_R = \frac{P_T G^2 \lambda^2 \sigma}{(4\pi)^2 r^4} \tag{53}$$

where P_T is the peak transmit power, G is the one-way power gain of the antenna, λ is the wavelength, r is the range, and σ is the radar cross section (RCS) of the point scatterer. We assume that the antenna boresight is pointing at the scatterer.

The power density at the receive antenna is

$$p_d = P_R/A_e \tag{54}$$

where A_e is the effective area of the receive antenna. Since $G = 4\pi A_e/\lambda^2$, we can write

$$p_d = \frac{P_T G\sigma}{(4\pi)^2 r^4} \tag{55}$$

Now let D be the distance from the RFSS array to the missile. If we radiate a power P_e from the array the power density at the receive antenna will be

$$p_d = P_e/4\pi D^2 \tag{56}$$

By equating (55) and (56) we obtain the effective radiated power as

$$P_e = \frac{P_r G D^2 \sigma}{4\pi r^4} \tag{57}$$

4. GENERATING THE MODULATION SIGNALS

In Section 3 a ray has been computed to each scatterer of the extended target model at one instant of time. The information comput ch scatterer is range, range rate, two angles, and an amplitude. In this section we will generate the modulation signals on the basis of the phasor summation of the component rays. The procedure is based on a constant-Doppler assumption for each scatterer during the interval between updates (the time between calculations of range, range rate, and amplitude for each scatterer).

4.1 Delay and Doppler Coefficients of Each Scatterer

Regardless of the approach used to generate the modulation signals, one must begin with the location of each scatterer in radar coordinates. In the notation of Section 3 the round-trip delay of the k^{th} scatterer is given by

$$\tau_k = 2(r_o + \Delta r_k)/c \tag{58}$$

where r_o is the range to the target c.g., Δr_k is the differential range of the k^{th} scatterer, and c is the propagation velocity. Even though the scatterers may be moving between updates we will assume that the radar is incapable of measuring this motion on the basis of its range resolution capability so that (58) can be assumed to be a constant that will be updated periodically.

The Doppler frequency of the k^{th} scatterer is given similarly by

$$\nu_k = -2(\dot{r}_o + \Delta\dot{r}_k)/\lambda \tag{59}$$

where $\dot{r}_o$ is the range rate of the target c.g., $\Delta\dot{r}_k$ is the differential Doppler of the k^{th} scatterer, and λ is the wavelength. Even though the scatterers may be accelerating between updates we will also assume that the radar is incapable of measuring this motion on the basis of its Doppler resolution capability. Thus (59) can be assumed to also be a constant that will be updated periodically.

4.2 The Exact Approach

For the moment, let us ignore the discussion in Section 2 on the medium-range target model. Instead, let us assume that we can apply an arbitrary delay and angular position in space to every scatterer in the target model (such an implementation would be straightforward in a nonreal-time digital simulation). Then if A_k represents the amplitude of the k^{th} scatterer, the instantaneous phasor assigned to the k^{th} scatterer is given by

$$V_k = A_k \, e^{j2\pi(\tau_k + \nu_k t)} \tag{60}$$

Note that if A_k^2 has the dimensions of RCS, then $|V_k|^2$ does also.

An implementation of this "exact" approach requires a separate signal generator for each scatterer. The delay and Doppler of each signal are given by (58) and (59), and the angular position in space of the k^{th} scatterer relative to the target c.g. is given by $(-\Delta b_k/r_o, -\Delta c_k/r_o)$, where Δb_k and Δc_k are defined in Section 3.

Since this approach is not capable of being implemented on the RFSS, at least when the number of scatterers is large, we will now concentrate on one method that is practical.

4.3 The Tapped-Delay Line Approach

The principal problem with the exact approach is that the scatterers can occur at arbitrary delays. It is a problem not only for generating analog signals, but also in an efficient implementation of a digital simulation. We solve this problem by constraining the scatterers to occur at one of a set of discrete times in delay that are uniformly spaced. But in solving one problem we create another.

If we move a scatterer in delay from its original value in (58) to some other value, the radar may be able to sense (measure) the change, especially if the sample spacing of the discrete delays is not small relative to the measurement accuracy of the radar (as will be the case in any practical implementation). Thus one cannot simply move the scatterer without changing the resulting response in the radar. However, one can implement a resampling technique that is described in Reference 1 (Section 5).

This technique is best viewed with respect to Figure 10, where four taps of a tapped delay line are located in delay about the delay of the scatterer of interest, two taps on each side of the scatterer. We will create new signals at these taps so that if the range gate in the receiver is centered at the delay of any one of these taps, the receiver will measure the same response as it would for the original scatterer. To find these four signals, which we designate as ω_i, $i=1, \ldots, 4$, let us define the range gate response amplitude, $\chi(\tau)$, to be a function of delay normalized to the tap spacing. Then if p is the differential delay between the second tap and the original scatterer we can write four equations as

$$\chi(1+p) = \omega_1\chi(0) + \omega_2\chi(1) + \omega_3\chi(2) + \omega_4\chi(3) \qquad (61)$$

$$\chi(p) = \omega_1\chi(-1) + \omega_2\chi(0) + \omega_3\chi(1) + \omega_4\chi(2) \qquad (62)$$

$$\chi(1-p) = \omega_1\chi(-2) + \omega_2\chi(-1) + \omega_3\chi(0) + \omega_4\chi(1) \qquad (63)$$

$$\chi(2-p) = \omega_1\chi(-3) + \omega_2\chi(-2) + \omega_3\chi(-1) + \omega_4\chi(0) \qquad (64)$$

In other words, the left side of (61) represents the amplitude weighting that would be placed on the original scatterer if the range gate were centered on the first tap, while the right side represents the composite weighting that would be applied to the four signals originating at the taps. We can solve

$\{\omega_1, \ldots, \omega_4\}$ = tap weights

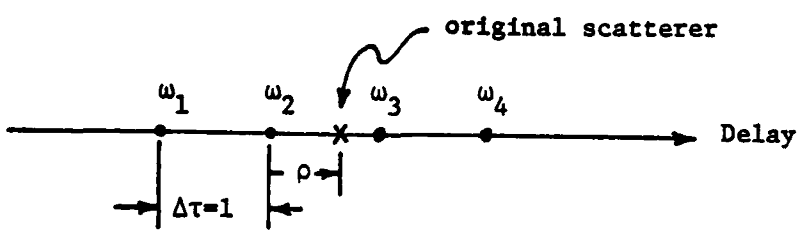

Figure 10. Creation of Signals at Four Taps of Tapped-Delay Line

this set of equations for ω_1 through ω_4, and the solution will apply to a specific value of p. The solution obtained in (61) through (64) is valid as long as the tap spacing is about 50% of the range gate spacing in the radar. We also assume that the range gate response drops off sufficiently fast so that no more than four taps (and four equations) need be evaluated.

4.4 Accumulation of Signals at Each Tap

At each tap three signals are formed, where each signal is a weighted summation of the phasors V_k defined by (60). The first signal for the n^{th} tap is the scintillation signal given by

$$V(n) = \sum_k V_k \omega_{n-\ell+1}(p) e^{-j4\pi(\ell-n+1+p)\Delta R_T/\lambda} \tag{65}$$

where the summation is over the set of scatterers, ΔR_T is the tap spacing in range units ($\Delta R_T = c\Delta\tau_T/2$ where $\Delta\tau_T$ is the delay between taps), ℓ is the tap number for the first of four that surround the k^{th} scatterer, and p is the fractional distance the k^{th} scatterer is from the second of four taps that surround the scatterer. The tap weights ω_i are nonzero only for $i=1,\ldots,4$. The phase factor in (65) is to compensate for the fact that the original scatterer is replaced by other components at different ranges.

The second signal for the n^{th} tap is the angle-weighted response in the horizontal direction (oriented to the RFSS chamber, or the B-direction in the notation of Section 3.4). It is given by

$$V_B(n) = \frac{1}{r_o} \sum_k \Delta b_k V_k \omega_{n-\ell+1}(p) e^{-j4\pi(\ell-n+1+p)\Delta R_T/\lambda} \tag{66}$$

The third signal is the angle-weighted response in the vertical direction (oriented to the RFSS chamber) and it is given by

$$V_C(n) = \frac{1}{r_o} \sum_k \Delta c_k V_k \omega_{n-\ell+1}(p) e^{-j4\pi(\ell-n+1+p)\Delta R_T/\lambda} \tag{67}$$

4.5 Computation of Glint Offsets at Each Tap

The angular glint offsets for each tap are computed as

$$\Delta_{AZ}(n) = -\mathrm{Re}\{V_B(n)/V(n)\} \tag{68}$$

$$\Delta_{EL}(n) = -\mathrm{Re}\{V_C(n)/V(n)\} \tag{69}$$

where we define the azimuth glint offset $\Delta_{AZ}(n)$ to be positive in the right-hand horizontal direction (referenced to the RFSS chamber, or in the negative B-direction), and elevation glint offset $\Delta_{EL}(n)$ to be positive up (or in the negative C-direction).

5. SIMULATION ARCHITECTURE

The computer resources that are available at the RFSS to generate extended target signals consist of a Datacraft/1 minicomputer that acts as a host to the AP120B array processor built by Floating Point Systems. The input to the host computer consists of the state of the engagement geometry and the output of the AP120B consists of the Doppler modulation signal and glint offsets at each tap ($V(n)$, $\Delta_{AZ}(n)$, $\Delta_{EL}(n)$). In deciding which operations are to be assigned to the two processors, the following factors were applied:

1) the array processor works best on arrays where the number of operations on each sample is few;
2) the program construction is costly for the array processor so that program should be fairly stable;
3) modifications are best made in the host computer; and
4) there should be relatively little traffic over the real-time interface between the host computer and the array processor.

With these factors in mind, the assignment of the various processing steps to generate extended target signals reduces naturally to:

<u>The host computer</u>

1. transform engagement geometry
2. compute visibility and amplitude of scatterers*

<u>The array processor</u>

1. compute which taps are affected by each scatterer
2. compute tap weights
3. compute and sum phasors at output sample rate
4. compute the Doppler modulation signal and glint offsets at each tap

*In some cases the computation for the amplitude of the scatterers might be too long for implementation in the host computer. In such a case, this computation can be transferred to the AP120B.

26 P.r.k

The real-time interface between the host and the AP120B consists of r_o and r_1, the range to the target c.g. and the range to the first tap; Δa_i, $\Delta \dot{a}_i$, Δb_i, and Δc_i, the ABC vector components for each visible scatterer; and A_i, the amplitude of the i^{th} scatterer.

In Appendix B we describe and give listings for an extended target simulation program that conforms to the above architecture.

References

1. Mitchell, R. L., and I. P. Bottlik, "Design Requirements for Simulating Realistic RF Environment Signals on the RFSS," MRI Report 132-44, 23 Sept. 1977.

2. Mott, H., "Three Channel Extended Target Model," RFSS Task 2 Technical Note 32, 15 July 1977.

This Page Intentionally Left Blank

APPENDIX A

LIMITING RANGE FOR MEDIUM-RANGE TARGET MODEL

Introduction

A medium-range target model was developed in Reference 1, consisting of N point scatterers, where each scatterer can have an RCS that is aspect dependent. The medium-range constraint assumes that all scatterers on the target are in the linear region of the monopulse receive beam, and all scatterers are illuminated with a constant gain by the transmit beam. The purpose of this constraint is to remove the sensor pointing angles from the real-time computation. In other words, the signal that is generated on the RFSS array is independent of the sensor pointing angles. At shorter ranges where the transmit beam is no longer uniform across the target, or where the monopulse difference beam is not linear, the pointing angles of the sensor beam must be known so that the variable weighting can be implemented in the real-time simulation; moreover, the signals that would be received on each monopulse channel must be separately simulated and radiated into specific points on the receive beam so that each channel receives the proper signal and rejects the others.[1]

The purpose of this memo is to determine the minimum range for the applicability of the medium-range model. A simple Monte-Carlo simulation will be used to accomplish this.

The Target Model

A statistical type target model is assumed. Two scatterers are separated by an angle θ_T, in between N-2 scatterers are placed at random. Thus the

[1] "Design Requirements for Simulating Realistic RF Environment Signals on the RFSS," MRI Report 132-44, by R. L. Mitchell and I. P. Bottlik, dated 23 September 1977.

target consists of N scatterers that cover an angular width of θ_T. All scatterers are assumed to be of equal RCS on the average, and each is fluctuated with a Rayleigh amplitude and random phase.

The Antenna Patterns

The sum channel two-way voltage antenna pattern is assumed to be

$$G_\Sigma(\theta) = 1 - \beta\theta^2 \tag{1}$$

and the two-way difference pattern

$$G_\Delta(\theta) = k(\theta - \alpha\theta^3) \tag{2}$$

Therefore, if the complex voltage is V_i on the ith scatterer at an angle θ_k, then the received voltages on the two channels are

$$V_\Sigma = \sum_i (1-\beta\theta_i^2)V_i \tag{3}$$

$$V_\Delta = k\sum_i (\theta_i - \alpha\theta_i^3)V_i \tag{4}$$

For the purpose of this investigation we have assumed

$$\alpha = 1.70/\theta_{3dB}^2 \tag{5}$$

$$\beta = 1.37/\theta_{3dB}^2 \tag{6}$$

where θ_{3dB} is the one-way half-power beamwidth. These values are typical of many tracking radars. The constant k will factor out of the problem later.

The Estimate of Angle

We assume that the boresite of the antenna is pointing exactly at the center of the target (midway between the end points). The estimate of angle is assumed to be

$$\hat{\theta}_{ACT} = \frac{1}{k}\,\mathrm{Re}\{V_\Delta/V_\Sigma\} \tag{7}$$

where the subscript ACT denotes the actual (assumed) target, in contrast to an approximate one based on the medium range model.

The Medium-Range Model

A glint centroid will be calculated for the target that is based on $G_\Sigma(\theta) = 1$ and $G_\Delta(\theta) = \theta$. Thus the composite signal

$$V' = \sum_i V_i \tag{8}$$

will be radiated from the angle

$$\theta' = \mathrm{Re}\left\{\frac{1}{V'}\sum_i \theta_i V_i\right\} \tag{9}$$

Now if we use the antenna patterns in (1) and (2), and the formula for the estimate of the angle, we have

$$\hat{\theta}_{APP} = \theta' \, \frac{1-\alpha(\theta')^2}{1-\beta(\theta')^2} \tag{10}$$

Thus we will compare $\hat{\theta}_{APP}$ with $\hat{\theta}_{ACT}$ to determine where the medium range model breaks down.

Results

In Tables A-1 through A-6 we show the results of 20 statistical replications of a target consisting of N=5 scatterers, where the target width varies from

θ_T/θ_{3dB} = .25 to 1.50 (the glint angles $\hat{\theta}_{ACT}$ and $\hat{\theta}_{APP}$ are designated as ACTUAL and APPROX, each being normalized to the half-power width). For a target width of 25% of the beamwidth (Table A-1) the peak error is .003 (or .3% of the beamwidth), which is negligible. For a target width of 50% of the beamwdith (Table A-2) the peak error is over 100% of the beamwidth (REP 20); however, the actual glint for this case is also large, amounting to 66% of the beamwidth. In practice, we can tolerate a large error if the glint angle is also large. It is more important to keep the errors small when the glint angles are small. Thus REP 12 in Table A-2 represents probably the most severe error, which is 2.8% of the beamwidth when the actual glint is 14% of the beamwidth.

If we rule out those replications where the actual glint is larger than half of the target width, we can construct the following table

Target Width	Peak Error
.25	.002
.50	.028
.75	.076
1.00	.184

All of these errors are negligible. However, when we go to a target of width $1.25\theta_{3dB}$ (Table A-5) we observe several large errors, even when the actual glint is small. For example, on REP 16 the actual glint is only 7.7% of the beamwidth, but the error is over 2 beamwidths. Clearly, the model breaks down for $\theta_T = 1.25\theta_{3dB}$. The actual point at which the model breaks down lies somewhere between $\theta_T = 1.00\theta_{3dB}$ and $\theta_T = 1.25\theta_{3dB}$. Variations in the antenna patterns and formulas for measuring angle will impact on a precise determination of where the model breaks down, but we can state conservatively that the model is valid as long as $\theta_T \lesssim \theta_{3dB}$.

In order to test the effect of the number of scatterers in the model, we repeated the previous simulation for N=10. The results are shown in Tables A-7 through A-12. No major discrepancies are noted from the previous conclusions.

Table A-1. Comparison of Actual Target with Medium-Range Model (APPROX) for θ_T/θ_{3dB} = 0.25 (N=5, all angles normalized to θ_{3dB})

REP	ACTUAL	APPROX	DIFF	.......SCATTERER	LOCATION.......			
1	.051	.051	-.000	-.125	.020	.072	.113	.125
2	-.057	-.058	-.001	-.125	-.123	-.051	-.012	.125
3	.043	.043	.000	-.125	-.056	-.049	.047	.125
4	-.074	-.073	.001	-.125	-.092	-.029	.083	.125
5	-.175	-.178	-.003	-.125	-.100	-.056	.021	.125
6	.167	.165	-.001	-.125	-.104	.030	.123	.125
7	.168	.169	.001	-.125	.048	.109	.120	.125
8	.002	.002	-.000	-.125	-.092	-.072	.091	.125
9	.015	.015	.000	-.125	-.120	.010	.080	.125
10	-.018	-.019	-.000	-.125	-.046	.066	.110	.125
11	.041	.041	.000	-.125	-.053	.021	.101	.125
12	.095	.096	.001	-.125	-.026	-.001	.097	.125
13	-.045	-.047	-.002	-.125	.024	.093	.108	.125
14	.085	.085	.000	-.125	-.073	-.009	.097	.125
15	-.069	-.071	-.002	-.125	-.013	-.011	.032	.125
16	-.035	-.034	.001	-.125	-.066	.023	.066	.125
17	.077	.077	-.000	-.125	-.014	-.001	.105	.125
18	-.109	-.110	-.001	-.125	-.087	-.072	.083	.125
19	.113	.114	.000	-.125	.044	.087	.107	.125
20	-.006	-.006	.000	-.125	-.062	-.055	-.035	.125

Table A-2. Comparison of Actual Target with Medium-Range Model (APPROX) for θ_T/θ_{3dB} = 0.50 (N=5, all angles normalized to θ_{3dB})

REP	ACTUAL	APPROX	DIFF	.......SCATTERER	LOCATION.......			
1	-.096	-.102	-.006	-.250	-.203	-.094	-.061	.250
2	-.042	-.054	-.011	-.250	.005	.075	.083	.250
3	-.220	-.208	.012	-.250	-.192	-.156	-.057	.250
4	.122	.126	.004	-.250	.105	.111	.176	.250
5	-.940	-1.774	-.835	-.250	-.242	-.214	.071	.250
6	-.459	-.445	.014	-.250	-.056	-.039	.227	.250
7	-.172	-.171	.001	-.250	-.212	.052	.199	.250
8	.116	.110	-.006	-.250	.036	.038	.204	.250
9	-.263	-.277	-.014	-.250	-.189	.045	.142	.250
10	.057	.063	.006	-.250	-.133	-.111	-.024	.250
11	.047	.044	-.003	-.250	-.181	.062	.152	.250
12	.141	.113	-.028	-.250	.008	.067	.120	.250
13	.088	.087	-.001	-.250	.004	.101	.124	.250
14	.031	.036	.004	-.250	-.076	-.007	.031	.250
15	-.666	-.400	.266	-.250	-.229	.150	.188	.250
16	.381	.364	-.017	-.250	.177	.177	.199	.250
17	-.305	-.284	.021	-.250	-.149	.001	.094	.250
18	.032	.040	.008	-.250	-.158	-.101	.179	.250
19	.075	.076	.001	-.250	-.189	-.141	.156	.250
20	.662	1.777	1.115	-.250	.018	.039	.227	.250

Table A-3. Comparison of Actual Target with Medium-Range Model (APPROX) for $\theta_T/\theta_{3dB} = 1.25$ (N=5, all angles normalized to θ_{3dB})

REP	ACTUAL	APPROX	DIFF	.......SCATTERER LOCATION.......				
1	-.315	-.332	-.017	-.625	-.549	-.540	-.369	.625
2	-.217	-.079	.138	-.625	-.453	-.304	.399	.625
3	1.017	-2.253	-3.271	-.625	-.558	-.303	-.230	.625
4	.229	.245	.016	-.625	-.549	.170	.410	.625
5	.038	-.007	-.045	-.625	-.240	.028	.241	.625
6	.459	.257	-.202	-.625	-.227	.348	.516	.625
7	-.118	-.032	.086	-.625	-.220	-.062	.110	.625
8	-.394	-1.867	-1.473	-.625	-.573	-.105	.085	.625
9	-.054	-.089	-.036	-.625	-.524	.033	.192	.625
10	.535	3.309	2.774	-.625	.136	.188	.561	.625
11	.496	.241	-.255	-.625	.158	.508	.553	.625
12	.222	-.131	-.352	-.625	-.211	.286	.466	.625
13	-.429	1.867	2.296	-.625	-.363	-.135	.105	.625
14	-.051	.216	.267	-.625	-.211	-.098	.439	.625
15	.005	.152	.147	-.625	-.253	-.173	.082	.625
16	.077	2.483	2.406	-.625	-.205	.024	.550	.625
17	-1.712	-.279	1.433	-.625	-.150	.068	.156	.625
18	-.400	-.453	-.053	-.625	-.377	-.302	-.271	.625
19	.010	.018	.007	-.625	-.032	.028	.605	.625
20	-.260	-.384	-.124	-.625	-.584	-.216	-.073	.625

Table A-4. Comparison of Actual Target with Medium-Range Model (APPROX) for $\theta_T/\theta_{3dB} = 1.50$ (N=5, all angles normalized to θ_{3dB})

REP	ACTUAL	APPROX	DIFF	.......SCATTERER LOCATION.......				
1	.476	-.155	-.631	-.750	-.294	.204	.466	.750
2	.139	-.236	-.375	-.750	-.634	-.299	.029	.750
3	-.091	14.613	14.704	-.750	-.542	-.200	.463	.750
4	-.093	2.506	2.598	-.750	-.518	-.348	.004	.750
5	-.138	-.129	.009	-.750	-.544	-.352	-.030	.750
6	.034	-.245	-.280	-.750	-.637	-.264	.575	.750
7	-.064	.343	.407	-.750	-.296	.097	.380	.750
8	-1.985	-.294	1.691	-.750	-.510	.558	.618	.750
9	.090	-.026	-.117	-.750	-.264	-.009	.398	.750
10	.229	-.016	-.245	-.750	-.309	.302	.347	.750
11	-.351	1.839	2.190	-.750	-.471	-.379	.746	.750
12	-.160	.288	.448	-.750	-.302	.676	.683	.750
13	-.396	-2.593	-2.198	-.750	-.548	.535	.598	.750
14	.261	1.782	1.521	-.750	-.641	-.018	.679	.750
15	.155	1.781	1.626	-.750	-.686	.555	.704	.750
16	.982	-8.846	-9.829	-.750	-.691	-.147	.341	.750
17	-.028	1.826	1.854	-.750	-.266	-.232	.749	.750
18	.023	-.221	-.244	-.750	-.743	-.295	.678	.750
19	-.005	.433	.438	-.750	-.708	-.016	.748	.750
20	-.352	-.301	.051	-.750	-.479	.386	.740	.750

Table A-5. Comparison of Actual Target with Medium-Range Model (APPROX) for θ_T/θ_{3dB} = .75 (N=5, all angles normalized to θ_{3dB})

REP	ACTUAL	APPROX	DIFF	.......SCATTERER	LOCATION.......			
1	-.981	-1.775	-.794	-.375	-.103	.108	.173	.375
2	-.470	-.454	.016	-.375	-.087	.004	.290	.375
3	.186	.171	-.015	-.375	-.278	.198	.286	.375
4	.258	.284	.025	-.375	-.319	.199	.312	.375
5	.317	.331	.013	-.375	.005	.016	.199	.375
6	.345	.346	.001	-.375	.314	.339	.343	.375
7	.675	.443	-.232	-.375	-.134	.188	.228	.375
8	.154	.181	.027	-.375	-.112	.252	.309	.375
9	.223	.253	.030	-.375	-.031	.032	.226	.375
10	-.168	-.180	-.013	-.375	-.154	-.118	.276	.375
11	.235	.311	.076	-.375	-.339	-.233	.150	.375
12	.201	.214	.013	-.375	-.325	-.311	.180	.375
13	.163	.172	.010	-.375	-.295	-.006	.022	.375
14	-.023	-.013	.009	-.375	-.348	-.236	-.096	.375
15	-.103	-.113	-.010	-.375	.092	.146	.315	.375
16	.435	.438	.003	-.375	.072	.334	.342	.375
17	.040	.045	.004	-.375	-.197	-.122	.018	.375
18	1.826	8.418	6.592	-.375	-.064	.067	.096	.375
19	.114	.151	.036	-.375	-.232	-.041	.128	.375
20	.261	.291	.030	-.375	.017	.077	.079	.375

Table A-6. Comparison of Actual Target with Medium-Range Model (APPROX) for θ_T/θ_{3dB} = 1.00 (N=5, all angles normalized to θ_{3dB})

REP	ACTUAL	APPROX	DIFF	.......SCATTERER	LOCATION.......			
1	-.170	-.128	.042	-.500	-.352	-.230	.350	.500
2	.129	.174	.044	-.500	-.194	-.122	.005	.500
3	.288	.336	.048	-.500	-.319	-.237	.316	.500
4	.172	.356	.184	-.500	-.497	-.198	.481	.500
5	-.289	-.277	.012	-.500	-.448	-.282	-.207	.500
6	-.247	-.300	-.053	-.500	-.395	.024	.037	.500
7	.230	.182	-.048	-.500	-.454	.090	.247	.500
8	-.438	-.437	.001	-.500	-.434	-.424	-.091	.500
9	-.114	-.252	-.138	-.500	-.096	-.058	.295	.500
10	1.003	1.775	.772	-.500	-.089	-.061	.259	.500
11	.221	.216	-.005	-.500	-.380	.057	.112	.500
12	.569	.071	-.499	-.500	-.299	.154	.227	.500
13	-.018	-.004	.015	-.500	-.410	-.150	.438	.500
14	.352	.221	-.130	-.500	-.221	-.052	.492	.500
15	.149	.098	-.050	-.500	-.346	-.313	.180	.500
16	-.397	-.326	.071	-.500	-.377	.295	.455	.500
17	-.341	-.369	-.028	-.500	-.476	-.078	.178	.500
18	-.116	-.097	.020	-.500	-.466	-.226	.081	.500
19	.264	.363	.099	-.500	-.336	-.294	.098	.500
20	.398	.416	.018	-.500	-.161	-.152	.309	.500

Table A-7. Comparison of Actual Target with Medium-Range Model (APPROX) for θ_T/θ_{3dB} = .25 (N=10, all angles normalized to θ_{3dB})

REP	ACTUAL	APPROX	DIFF
1	.014	.014	.001
2	.033	.033	.000
3	-.029	-.029	.000
4	.042	.042	-.000
5	.032	.031	-.001
6	-.007	-.007	.000
7	-.000	-.000	-.000
8	-.014	-.006	.007
9	.010	.010	-.000
10	-.092	-.096	-.003
11	-.023	-.023	.000
12	.139	.138	-.001
13	.046	.047	.001
14	.042	.042	.000
15	-.055	-.057	-.001
16	.018	.019	.001
17	.003	.003	-.000
18	-.118	-.117	.000
19	-.136	-.139	-.003
20	-.056	-.058	-.002

Table A-8. Comparison of Actual Target with Medium-Range Model (APPROX) for θ_T/θ_{3dB} = .50 (N=10, all angles normalized to θ_{3dB})

REP	ACTUAL	APPROX	DIFF
1	.049	.060	.011
2	.040	.048	.008
3	.167	.178	.011
4	.242	.272	.030
5	.177	.191	.014
6	.042	.042	-.000
7	-.110	-.108	.002
8	-.038	-.045	-.006
9	.032	.037	.005
10	1.030	1.792	.762
11	-.039	-.049	-.009
12	.111	.122	.010
13	-.156	-.147	.009
14	.161	.167	.006
15	-.052	-.055	-.002
16	-.206	-.218	-.012
17	.028	.027	-.001
18	-.217	-.208	.009
19	-.095	-.098	-.004
20	-.121	-.103	.018

Table A-9. Comparison of Actual Target with Medium-Range Model (APPROX) for θ_T/θ_{3dB} = .75 (N=10, all angles normalized to θ_{3dB})

REP	ACTUAL	APPROX	DIFF
1	-.049	-.043	.006
2	.017	.000	-.016
3	.022	.026	.004
4	-.141	-.142	-.001
5	.542	.451	-.092
6	-.083	-.111	-.028
7	.021	.023	.002
8	.226	.108	-.118
9	1.156	1.825	.669
10	.188	.224	.036
11	-.043	-.043	.000
12	.282	.356	.074
13	.055	.053	-.001
14	.119	.093	-.026
15	.192	.228	.036
16	-.232	-.303	-.072
17	.587	.036	-.551
18	.247	.291	.043
19	.036	.031	-.005
20	-.309	-.299	.010

Table A-10. Comparison of Actual Target with Medium-Range Model (APPROX) for θ_T/θ_{3dB} = 1.00 (N=10, all angles normalized to θ_{3dB})

REP	ACTUAL	APPROX	DIFF
1	-.045	-.096	-.051
2	.048	.068	.020
3	-.013	.003	.016
4	.681	2.162	1.481
5	-.426	-.442	-.016
6	.327	.364	.037
7	-.045	-.128	-.083
8	.129	.232	.103
9	-.411	-.458	-.047
10	.055	.077	.022
11	-.173	-.073	.100
12	.143	.124	-.019
13	.292	.391	.099
14	-.109	-.154	-.045
15	.224	.314	.090
16	-.201	-.227	-.025
17	.462	.459	-.003
18	-.346	-.366	-.020
19	.203	.414	.211
20	-.036	-.021	.015

Table A-11. Comparison of Actual Target with Medium-Range Model (APPROX) for θ_T/θ_{3dB} = 1.25 (N-10, all angles normalized to θ_{3dB})

REP	ACTUAL	APPROX	DIFF
1	-.220	-.220	-.001
2	.368	.402	.034
3	-.271	-.365	-.094
4	.077	.138	.061
5	.187	-.258	-.445
6	-.184	-.455	-.271
7	.027	1.922	1.895
8	-.006	-.082	-.076
9	-.284	-.356	-.072
10	-.155	-.233	-.078
11	-.811	-2.001	-1.190
12	-.229	-.277	-.048
13	.248	.216	-.032
14	.041	-.025	-.065
15	-.363	-.431	-.069
16	-.070	-.177	-.107
17	-.675	-3.174	-2.499
18	-.136	.441	.577
19	-.058	-.167	-.108
20	.375	.357	-.018

Table A-12. Comparison of Actual Target with Medium-Range Model (APPROX) for θ_T/θ_{3dB} = 1.50 (N=10, all angles normalized to θ_{3dB})

REP	ACTUAL	APPROX	DIFF
1	.153	.418	.265
2	.053	.156	.103
3	.800	.431	-.369
4	.242	.456	.214
5	-.165	.170	.335
6	.068	-.269	-.337
7	-.222	-.439	-.217
8	.155	.452	.297
9	.048	-.254	-.302
10	.017	.284	.268
11	.863	.095	-.768
12	.006	-2.603	-2.609
13	.179	-.085	-.263
14	.006	-.173	-.179
15	-.003	.145	.148
16	-.305	-1.774	-1.470
17	.019	-.447	-.466
18	.057	.213	.156
19	-.044	-.380	-.336
20	.140	.204	.064

APPENDIX B

FORTRAN PROGRAM FOR GENERATING REAL-TIME EXTENDED TARGET SIGNALS

The Fortran program described here generates the Doppler modulation signal and glint offsets at each tap of a tapped-delay line for an extended target composed of a set of discrete scatterers. It represents the latest version delivered to MIRADCOM on 20 June 1978, and only minor corrections in comment statements are made in the following listings, with the exception of subroutine XFORM (where the sign convention on all angles was reversed).

There are two principal subroutines in this program, TARGEO which computes the amplitude and geometrical information for each scatterer, and TARGDM which computes the Doppler modulation and glint offsets for each tap. This architecture assumes that TARGEO will be installed in the host computer and TARGDM in the AP120B array processor. Block diagrams for these two subroutines are sketched in Figures B-1 and B-2. The assignment of the other subroutines is as follows:

<u>Host Computer</u>

- MAIN - main or driver program
- ETGEO - updates and transforms engagement geometry
- XFORM - transforms inertial coordinates to target coordinates
- SCTAMP - computes amplitude of scatterer

<u>AP120B</u>

- ETGDM - generates Doppler modulation and glint offsets
- TAPWTS - compute tap weights (table lookup)

<u>Initialization (Host)</u>

- TAPSET - generates tap weight table (for TAPWTS)
- CHI - range gate response (used by TAPSET)
- SIMQ - simultaneous equation solution (used by TAPSET)
- DATAIN - reads target scattering data from cards

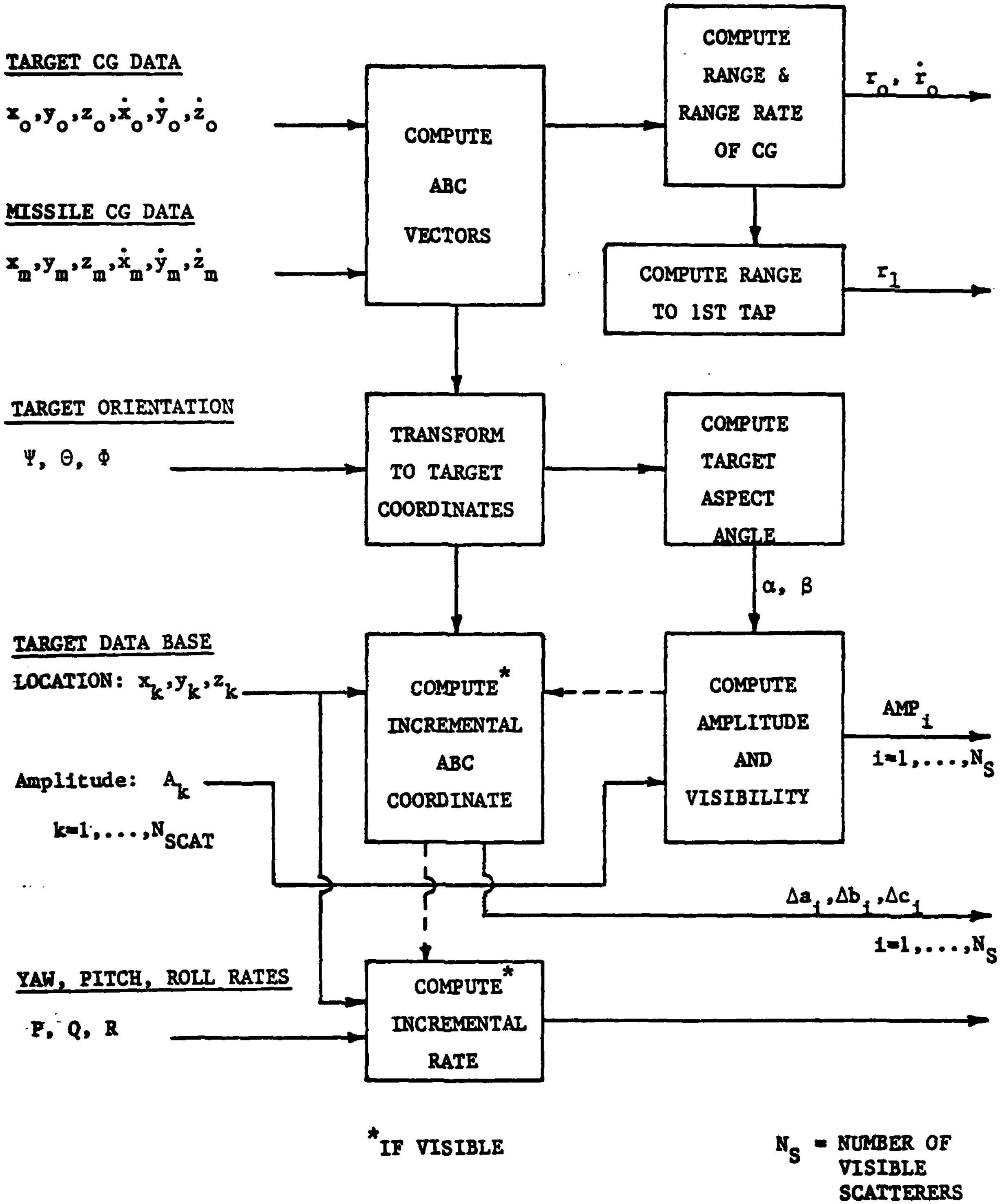

Figure B-1. BLOCK DIAGRAM FOR SUBROUTINE TARGEO
(computes amplitude & geometrical info for each scatterer)

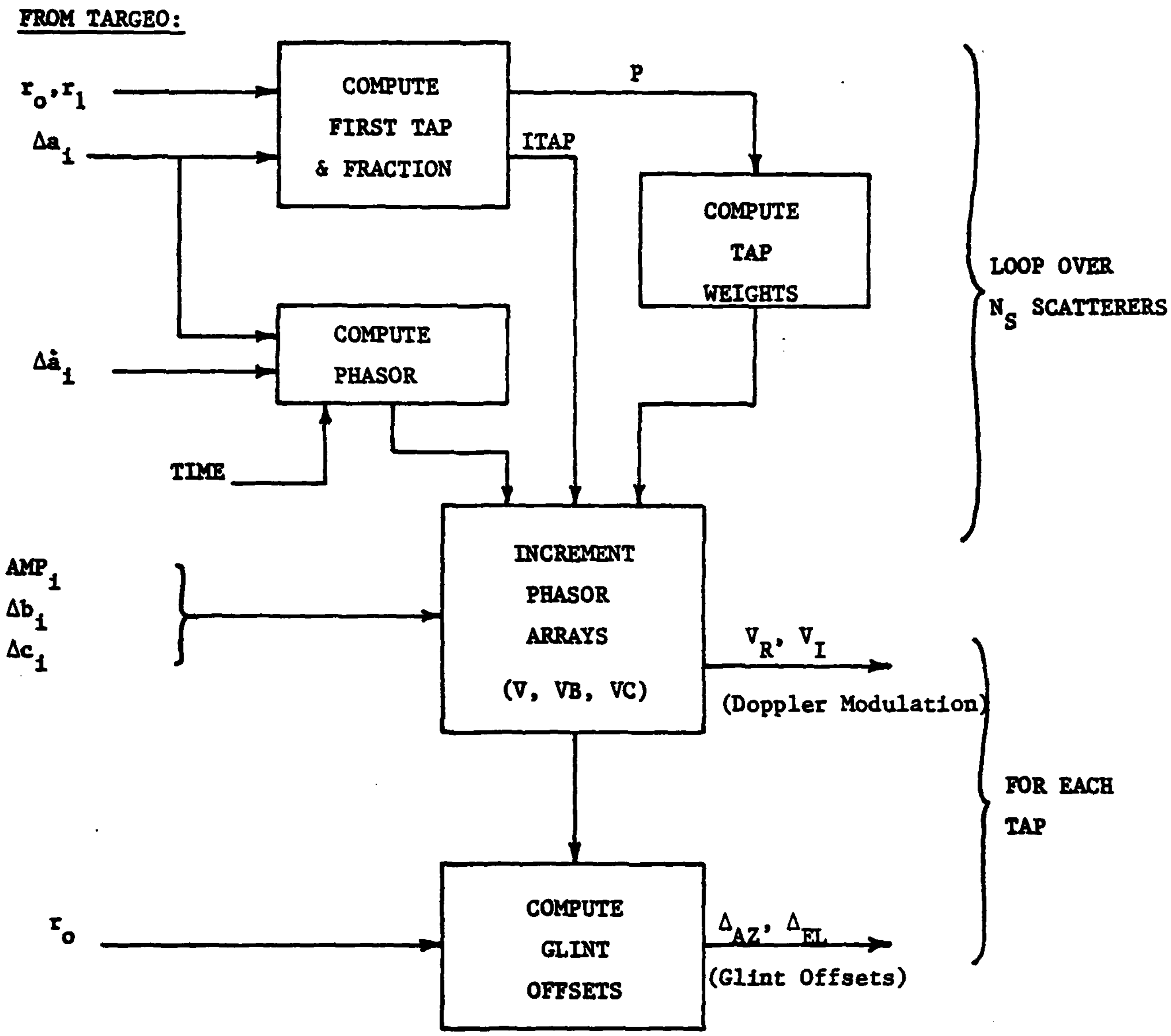

Figure B-2. BLOCK DIAGRAM FOR SUBROUTINE TARGDM
(computes Doppler modulation & glint offsets for each tap)

Utility

XMIT - moves data

SINCOS - computes sine/cos

A sample test program is included as MAIN in the following listings, and an alternate Doppler modulation and glint offset subroutine (ETGD1) is included that is based on a single tap (no range extent).

NOTE: The programs listed here for eventual installation on the AP120B are written in FORTRAN; they must be converted to the appropriate language on the SP120B in order to run in real time.

```
      PROGRAM MAIN (INPUT,OUTPUT,TAPE5=INPUT,TAPE6=OUTPUT)
C
C THIS IS A SAMPLE MAIN PROGRAM FOR TEST PURPOSES ONLY.
C
C THIS EXTENDED-TARGET SIMULATION PACKAGE HAS BEEN PREPARED BY
C RL MITCHELL OF MARK RESOURCES, INC (213-822-4955), UNDER CONTRACT TO
C MIRADCOM.  IT IS WRITTEN WITH THE INTENTION THAT IT WILL BE MADE PART
C OF A REAL-TIME SIMULATION PROGRAM, ALTHOUGH SOME OF THE CODE IS NOT
C WRITTEN IN COMPLETELY OPTIMUM FORM (IT IS MORE EASILY UNDERSTOOD THIS
C WAY, AND THE REVISIONS ARE EASILY MADE).
C
C ALL ARRAYS IN COMMON SHOULD BE DIMENSIONED IN THE MAIN PROGRAM.
C
C SEE THE SUBROUTINES FOR A DEFINITION OF THE VARIABLES.
C
C RULES FOR DIMENSIONING ARRAYS.....
C
C       X,Y,Z...............NSCAT
C       AMP,DA,DB,DC,DAD....NSCAT (MAYBE SMALLER)
C       TWARAY..............4*NARAY
C       VR,VI,DAZ,DEL.......NTAP
C
C
C
C
      COMMON /T1/ XO,YO,ZO,XOD,YOD,ZOD,PSI,THETA,PHI,BP,BQ,BR
      COMMON /T2/ CPSI,SPSI,CTHETA,STHETA,CPHI,SPHI
      COMMON /T3/ XM,YM,ZM,XMD,YMD,ZMD
      COMMON /T4/ NSCAT,ST,AMPMIN,X(20),Y(20),Z(20)
      COMMON /T5/ NTAP,DRTAP,DRGATE,XL,PTGDSQ
      COMMON /T6/ NARAY,TWARAY(404)
      COMMON /T7/ NS,RO,R1,ROD,AMP(20),DA(20),DB(20),DC(20),DAD(20)
      COMMON /T8/ PEFF,VR(8),VI(8),DAZ(8),DEL(8)
C
C DEFINE VARIABLES.....
C
      DATA LR,LW/5,6/
      DATA NTAP/8/,DRTAP/30./,DRGATE/60./,XL/.02/,AMPMIN/1.E-10/,
     1     PTGDSQ/1./
      DATA DTIME/1./
      DATA NARAY/101/
      DATA ST/0./

      READ  (LR,100) XO,YO,ZO
      READ  (LR,100) XOD,YOD,ZOD
      READ  (LR,100) PSI,THETA,PHI
      READ  (LR,100) BP,BQ,BR
      READ  (LR,100) XM,YM,ZM
      READ  (LR,100) XMD,YMD,ZMD
      READ  (LR,101) NSCAT
```

```
      READ  (LR,100) (X(K),Y(K),Z(K),K=1,NSCAT)

      WRITE (LW,200) XO,YO,ZO
      WRITE (LW,201) XOD,YOD,ZOD
      WRITE (LW,202) PSI,THETA,PHI
      WRITE (LW,203) BP,BQ,BR
      WRITE (LW,204) XM,YM,ZM
      WRITE (LW,205) XMD,YMD,ZMD
      WRITE (LW,206) NSCAT
      WRITE (LW,207) (X(K),Y(K),Z(K),K=1,NSCAT)
C
C SUBROUTINES TO BE CALLED FROM MAIN OR DRIVER PROGRAM.....
C
      CALL DATAIN

      CALL TAPSET

      CALL ETGEO

      CALL ETGDM(DTIME)

      WRITE (LW,208) RO,R1,ROD
      WRITE (LW,209) (AMP(K),DA(K),DB(K),DC(K),DAD(K),K=1,NS)
      WRITE (LW,210) DTIME
      WRITE (LW,211) (VR(I),VI(I),DAZ(I),DEL(I),I=1,NTAP)
      WRITE (LW,212) PEFF

      STOP

  100 FORMAT(3F10.1)
  101 FORMAT(I5)

  200 FORMAT(//14H XO,YO,ZO...../(20X3F12.6))
  201 FORMAT(//17H XOD,YOD,ZOD...../(20X3F12.6))
  202 FORMAT(//19H PSI,THETA,PHI...../(20X3F12.6))
  203 FORMAT(//14H BP,BQ,BR...../(20X3F12.6))
  204 FORMAT(//14H XM,YM,ZM...../(20X3F12.6))
  205 FORMAT(//17H XMD,YMD,ZMD...../(20X3F12.6))
  206 FORMAT(//11H NSCAT...../20XI12)
  207 FORMAT(//11H X,Y,Z...../(20X3F12.6))
  208 FORMAT(//15H RO,R1,ROD...../(20X3F12.6))
  209 FORMAT(//22H AMP,DA,DB,DC,DAD...../(20X5F12.6))
  210 FORMAT(//11H DTIME...../20XF12.6)
  211 FORMAT(//19H VR,VI,DAZ,DEL...../(20X4F12.6))
  212 FORMAT(//10H PEFF...../20XE12.5)
      END
```

```
      SUBROUTINE ETGEO
C
C TRANSFORMATION TO RADAR SPACE FOR N-POINT SCATTERER MODEL
C
C IN THIS SUBROUTINE WE BEGIN WITH THE MODEL OF AN EXTENDED TARGET AND
C THE ENGAGEMENT GEOMETRY IN ORDER TO COMPUTE THE AMPLITUDE AND RADAR
C COORDINATES FOR EACH SCATTERER IN THE MODEL.
C
C THE MODEL IMPLEMENTED IS THE SO-CALLED MEDIUM-RANGE MODEL (SEE MRI
C REPORT 132-44).
C
C ASSUMPTIONS AND LIMITATIONS.....
C
C             1. ALL SCATTERERS ASSUMED TO BE ILLUMINATED BY SAME TRANSMIT
C                ANTENNA GAIN.
C             2. TARGET ASSUMED TO BE WITHIN LINEAR REGION OF MONOPULSE
C                RECEIVE BEAM.
C             3. THE DOPPLER SHIFT OF THE TARGET CG IS IMPLEMENTED BY MEANS
C                OF A FINELY-CONTROLLABLE DELAY LINE (THE LASER DEVICE),
C                PLUS THE USE OF THE FREQUENCY SYNTHESIZER.
C             4. ONLY ONE PHYSICAL TARGET IS SIMULATED PER CALL.
C
C ALL COMMUNICATION TO AND FROM THIS SUBROUTINE IS THRU COMMON.
C
C ON INPUT.....
C
C       /T1/    XO,YO,ZO          = TARGET CG IN INERTIAL COORDINATES
C               XOD,YOD,ZOD       = TARGET CG RATE IN INERTIAL COORDINATES
C               PSI,THETA,PHI     = YAW, PITCH, ROLL ANGLES
C               BP,BQ,BR          = YAW, PITCH, ROLL ANGLE BODY RATES
C
C       /T3/    XM,YM,ZM          = MISSILE CG IN INERTIAL COORDINATES
C               XMD,YMD,ZMD       = MISSILE CG RATE IN INERTIAL COORDINATES
C
C       /T4/    NSCAT = NUMBER OF SCATTERERS IN TARGET MODEL
C               ST    = APPROXIMATE PHYSICAL SIZE OF TARGET
C               AMPMIN = AMPLITUDE THRESHOLD FOR SCATTERERS
C               X,Y,Z = ARRAYS CONTAINING SCATTERER LOCATIONS IN TARGET
C                       COORDINATES
C
C       /T5/    NTAP   = NUMBER OF TAPS IN TAPPED DELAY LINE
C               DRTAP  = SPACING BETWEEN TAPS       (RANGE)
C
C ON OUTPUT.....
C
C       /T2/    CPSI,SPSI,...ETC = SINES AND COSINES OF TARGET ANGLES
C
C       /T7/    NS     = NUMBER OF SCATTERERS VISIBLE
C               RO     = RANGE TO TARGET CG
C               R1     = RANGE TO FIRST TAP
```

```
C                 ROD    = RANGE RATE OF TARGET CG
C                 AMP(J) = AMPLITUDE OF J-TH SCATTERER
C                 DA(J)  = INCREMENTAL A-VECTOR OF J-TH SCATTERER
C                 DB(J)  = INCREMENTAL B-VECTOR OF J-TH SCATTERER
C                 DC(J)  = INCREMENTAL C-VECTOR OF J-TH SCATTERER
C                 DAD(J) = INCREMENTAL A-VECTOR RATE OF J-TH SCATTERER
C
C THE TARGET CG AND MISSILE CG COORDINATES ARE IN AN INERTIAL COORDINATE
C SYSTEM REFERENCED TO THE GROUND (XY-PLANE PARALLEL TO GROUND, Z- DOWN)
C
C THE ABC-VECTORS ARE DEFINED AS.....
C
C      A - FROM THE TARGET TO THE MISSILE
C      B - PARALLEL TO THE GROUND, TO THE LEFT AS VIEWED FROM MISSILE
C      C - PERPENDICULAR TO A AND B IN RIGHT-HAND COORDINATE SYSTEM
C
C THE TARGET COORDINATES ARE.....
C
C      X - TARGET LONGITUDINAL AXIS, POSITIVE IN DIRECTION OF NOSE
C      Y - IN DIRECTION OF RIGHT WING
C      Z - DOWN
C
C THE BODY RATES ARE DEFINED AS.....
C
C     BP - CW ROTATION RATE ABOUT TARGET X-AXIS
C     BQ - CW ROTATION RATE ABOUT TARGET Y-AXIS
C     BR - CW ROTATION RATE ABOUT TARGET Z-AXIS
C
C THE DIRECTION OF ROTATION IS DEFINED LOOKING OUT FROM THE COORDINATE
C ORIGIN.
C
C SEE SUBROUTINE XFORM FOR A DEFINITION OF THE YAW, PITCH, AND ROLL
C ANGLES.
C
C THE RFSS CHAMBER COORDINATES ARE ASSUMED TO BE PARALLEL TO THE ABC-
C VECTORS.  RANGE IS IN -A DIRECTION, RIGHT AZIMUTH IN -B DIRECTION, AND
C UP ELEVATION IN -C DIRECTION.
C
C ALL DISTANCES (INCLUDING WAVELENGTH) MUST BE IN THE SAME UNITS.  ALL
C ANGLES MUST BE IN RADIANS.
C
      DIMENSION A(3),B(3),C(3),WA(3),WB(3),WC(3)
      COMMON /T1/ XO,YO,ZO,XOD,YOD,ZOD,PSI,THETA,PHI,BP,BQ,BR
      COMMON /T2/ CPSI,SPSI,CTHETA,STHETA,CPHI,SPHI
      COMMON /T3/ XM,YM,ZM,XMD,YMD,ZMD
      COMMON /T4/ NSCAT,ST,AMPMIN,X(20),Y(20),Z(20)
      COMMON /T5/ NTAP,DRTAP
      COMMON /T7/ NS,RO,R1,ROD,AMP(20),DA(20),DB(20),DC(20),DAD(20)
C
C COMPUTE SINES AND COSINES OF ANGLES
```

```
C
      CALL SINCOS(PSI,SPSI,CPSI)
      CALL SINCOS(THETA,STHETA,CTHETA)
      CALL SINCOS(PHI,SPHI,CPHI)
C
C COMPUTE RANGE TO TARGET CG AND A-VECTOR
C
      A(1)=XM-XO
      A(2)=YM-YO
      A(3)=ZM-ZO
      RO=SQRT(A(1)**2+A(2)**2+A(3)**2)
      A(1)=A(1)/RO
      A(2)=A(2)/RO
      A(3)=A(3)/RO
C
C COMPUTE RANGE TO FIRST TAP
C
      R1=RO-.5*(NTAP-1)*DRTAP
C
C COMPUTE RANGE RATE OF TARGET CG
C
      ROD=A(1)*(XOD-XMD)+A(2)*(YOD-YMD)+A(3)*(ZOD-ZMD)
C
C COMPUTE B- AND C-VECTORS
C
      RHO=SQRT(A(1)**2+A(2)**2)
      B(1)=-A(2)/RHO
      B(2)= A(1)/RHO
      B(3)=0.
      C(1)=-A(3)*B(2)
      C(2)= A(3)*B(1)
      C(3)=RHO
C
C TRANSFORM A-, B-, AND C-VECTORS TO TARGET COORDINATES
C
      CALL XFORM(A,WA)
      CALL XFORM(B,WB)
      CALL XFORM(C,WC)
C
C COMPUTE TARGET ASPECT ANGLE (ALPHA=AZIMUTH, BETA=ELEVATION,
C                                 ANGL=ANGLE TO ROLL AXIS)
C
C     ALPHA=ATAN2(WA(2),WA(1))
C     SBETA=-WA(3)
C     BETA=ATAN2(SBETA,SQRT(1.-SBETA**2))
      ANGL=ATAN2(SQRT(1.-WA(1)**2),WA(1))
C
C LOOP OVER SCATTERERS
C
      L=1
```

```
      DO 20 K=1,NSCAT
      SAMP=SCTAMP(K,ANGL)
      IF(SAMP.LE.AMPMIN) GO TO 20
      AMP(L)=SAMP
C
C COMPUTE INCREMENTAL A,B,C COORDINATE
C
      DA(L)=X(K)*WA(1)+Y(K)*WA(2)+Z(K)*WA(3)
      DB(L)=X(K)*WB(1)+Y(K)*WB(2)+Z(K)*WB(3)
      DC(L)=X(K)*WC(1)+Y(K)*WC(2)+Z(K)*WC(3)
C
C COMPUTE INCREMENTAL A-VECTOR RATE (SMALL ANGLES ARE ASSUMED)
C
      XKD= Z(K)*BQ-Y(K)*BR
      YKD=-Z(K)*BP+X(K)*BR
      ZKD= Y(K)*BP-X(K)*BQ
      DAD(L)=XKD*WA(1)+YKD*WA(2)+ZKD*WA(3)
      L=L+1
   20 CONTINUE
      NS=L-1
      RETURN
      END
```

```
      SUBROUTINE ETGDM(DTIME)
C
C GLINT AND DOPPLER MODULATION FOR N-POINT SCATTER MODEL
C
C IN THIS SUBROUTINE WE COMPUTE THE GLINT OFFSETS AND MODULATION SIGNALS
C APPLIED TO EACK TAP OF THE TAPPED-DELAY LINE.  IT IS TO BE CALLED
C AFTER ETGEO TRANSFORMS COORDINATES TO RADAR SPACE.  IT WILL USUALLY
C BE CALLED MORE FREQUENTLY THAN ETGEO.  IT IS ALSO THE BEST SUBROUTINE
C TO PLACE IN THE AP120B.
C
C EXCEPT FOR TIME, ALL COMMUNICATION TO AND FROM THIS SUBROUTINE IS THRU
C COMMON.
C
C ON INPUT.....
C
C              DTIME  = TIME SINCE LAST UPDATE IN TARGEO
C
C       /T5/   NTAP   = NUMBER OF TAPS IN TAPPED DELAY LINE
C              DRTAP  = SPACING BETWEEN TAPS        (RANGE)
C              XL     = WAVELENGTH
C              PTGDSQ = PRODUCT OF TRANSMIT POWER, GAIN, AND SQUARE OF
C                       RFSS CHAMBER LENGTH
C
C       /T7/   NS     = NUMBER OF SCATTERERS VISIBLE
C              RO     = RANGE TO TARGET CG
C              R1     = RANGE TO FIRST TAP
C              AMP(J) = AMPLITUDE OF J-TH SCATTERER
C              DA(J)  = INCREMENTAL A-VECTOR OF J-TH SCATTERER
C              DB(J)  = INCREMENTAL B-VECTOR OF J-TH SCATTERER
C              DAD(J) = INCREMENTAL A-VECTOR RATE OF J-TH SCATTERER
C
C ON OUTPUT.....
C
C       /T8/   PEFF   = EFFECTIVE RADIATED POWER AT RFSS ARRAY
C              VR(I)  = IN-PHASE   MODULATION SIGNAL TO I-TH TAP
C              VI(I)  = QUADRATURE MODULATION SIGNAL TO I-TH TAP
C              DAZ(I) = GLINT OFFSET (AZIMUTH)   FOR I-TH TAP
C              DEL(I) = GLINT OFFSET (ELEVATION) FOR I-TH TAP
C
C THE PARAMETER PMIN IS JUST SOME SMALL NUMBER TO PREVENT DIVIDE BY ZERO
C
C ARRAYS VBR,VBI,VCR,VCI MUST BE DIMENSIONED AS LARGE AS NTAP
C
      DIMENSION VBR(8),VBI(8),VCR(8),VCI(8)
      DIMENSION SS(4),CC(4)
      DIMENSION TW(4)
      COMMON /T5/ NTAP,DRTAP,DRGATE,XL,PTGDSQ
      COMMON /T7/ NS,RO,R1,ROD,AMP(20),DA(20),DB(20),DC(20),DAD(20)
      COMMON /T8/ PEFF,VR(8),VI(8),DAZ(8),DEL(8)
      DATA PMIN/1.E-10/
```

```
      DATA FOURPI/12.5663706/
C
C ZERO ARRAYS
C
      CALL XMIT(-NTAP,0.,VR)
      CALL XMIT(-NTAP,0.,VI)
      CALL XMIT(-NTAP,0.,VBR)
      CALL XMIT(-NTAP,0.,VBI)
      CALL XMIT(-NTAP,0.,VCR)
      CALL XMIT(-NTAP,0.,VCI)
      CALL XMIT(-NTAP,0.,DAZ)
      CALL XMIT(-NTAP,0.,DEL)
C
C LOOP OVER NS SCATTERERS
C
      DO 40 J=1,NS
C
C COMPUTE TAP NUMBER OF FIRST TAP (ITAP) AND FRACTION (P)
C
      R=RO-(DA(J)+DAD(J)*DTIME)
      P=(R-R1)/DRTAP+100.
      ITAP=P
      P=P-ITAP
      ITAP=ITAP-100
C
C COMPUTE RANGE DIFFERENCE FROM TAP NUMBER ITAP
C
      DR=(P+1.)*DRTAP
C
C FIND TAP WEIGHTS
C
      CALL TAPWTS(P,TW)
C
C COMPUTE PHASE ON FOUR TAPS
C
      DO 20 I=1,4
      CALL SINCOS(-FOURPI*DR/XL,S,C)
      SS(I)=S*AMP(J)*TW(I)
      CC(I)=C*AMP(J)*TW(I)
      DR=DR-DRTAP
   20 CONTINUE
C
C LOOP OVER UP TO FOUR TAPS AND INCREMENT ARRAYS
C
      IF(ITAP.GT.NTAP) GO TO 40
      IF(ITAP.LT.-2)   GO TO 40
      I1=MAX0(ITAP,1)
      I2=MIN0(ITAP+3,NTAP)
      II=I1-ITAP
      DO 30 I=I1,I2
```

```
      II=II+1
      VR (I)=VR (I)+CC(II)
      VI (I)=VI (I)+SS(II)
      VBR(I)=VBR(I)+CC(II)*DB(J)
      VBI(I)=VBI(I)+SS(II)*DB(J)
      VCR(I)=VCR(I)+CC(II)*DC(J)
      VCI(I)=VCI(I)+SS(II)*DC(J)
   30 CONTINUE
   40 CONTINUE
C
C COMPUTE GLINT OFFSETS FOR EACH TAP AND PEAK POWER
C
      PEAK=0.
      DO 50 I=1,NTAP
      POW=VR(I)**2+VI(I)**2
      IF(POW.GT.PEAK) PEAK=POW
      IF(POW.LT.PMIN) GO TO 50
      DAZ(I)=-(VBR(I)*VR(I)+VBI(I)*VI(I))/(RO*POW)
      DEL(I)=-(VCR(I)*VR(I)+VCI(I)*VI(I))/(RO*POW)
   50 CONTINUE
C
C NORMALIZE AMPLITUDE
C
      ANORM=SQRT(PEAK)
      DO 60 I=1,NTAP
      VR(I)=VR(I)/ANORM
      VI(I)=VI(I)/ANORM
   60 CONTINUE
C
C COMPUTE EFFECTIVE RF POWER
C
      PEFF=PEAK*PTGDSQ/(FOURPI*RO**4)

      RETURN
      END
```

```
      SUBROUTINE XFORM(A,W)
C
C IN THIS SUBROUTINE WE TRANSFORM A VECTOR (A) IN INERTIAL COORDINATES
C TO A VECTOR (W) IN TARGET COORDINATES.  THE COORDINATE ROTATIONS, IN
C THE ORDER OF APPLICATION, ARE.....
C
C       PSI   = CW ROTATION OF Z-AXIS
C       THETA = CW ROTATION OF Y-AXIS
C       PHI   = CW ROTATION OF X-AXIS
C
C THE DIRECTION OF ROTATION IS DEFINED LOOKING OUT FROM THE COORDINATE
C ORIGIN.  IN THIS SUBROUTINE THE SINES AND COSINES OF THE ANGLES ARE
C INPUT THROUGH COMMON /T2/.
C
      DIMENSION A(3),W(3)
      COMMON /T2/ CPSI,SPSI,CTHETA,STHETA,CPHI,SPHI
      UX= A(1)*CPSI+A(2)*SPSI
      UY=-A(1)*SPSI+A(2)*CPSI
      UZ= A(3)
      VX= UX*CTHETA-UZ*STHETA
      VY= UY
      VZ= UX*STHETA+UZ*CTHETA
      W(1)= VX
      W(2)= VY*CPHI+VZ*SPHI
      W(3)=-VY*SPHI+VZ*CPHI
      RETURN
      END
```

```
      SUBROUTINE TAPWTS(P,TW)
C
C IN THIS SUBROUTINE FOUR TAP WEIGHTS ARE RETURNED IN ARRAY TW ACCORDING
C TO THE FRACTION P.  THE WEIGHTS ARE EXTRACTED FROM A PRECOMPUTED TABLE
C (SEE SUBROUTINE TAPSET).
C
C ARRAY TWARAY IS USED AS IF IT WERE DIMENSIONED (4,NARAY).
C
      DIMENSION TW(4)
      COMMON /T6/ NARAY,TWARAY(1)
      DATA LW/6/
      INDEX=(NARAY-1)*P+1.5
      CALL XMIT(4,TWARAY(4*INDEX-3),TW)
C
C
      RETURN
      END
```

```
      SUBROUTINE TAPSET
C
C IN THIS SUBROUTINE THE TAP WEIGHT TABLE IS COMPUTED.   IT IS A
C COMPANION SUBROUTINE TO TAPWTS, AND IT IS TO BE CALLED AS AN INITIAL-
C IZATION STEP PRIOR TO THE BEGINNING OF THE SIMULATED MISSION.
C
C       /T5/   DRTAP  = SPACING BETWEEN TAPS          (RANGE)
C              DRGATE = SPACING BETWEEN RECEIVER GATES          (RANGE)
C
C ARRAY TWARAY MUST BE DIMENSIONED AS LARGE AS 4*NARAY.
C
      DIMENSION A(4,4),X(4)
      COMMON /T5/ NTAP,DRTAP,DRGATE
      COMMON /T6/ NARAY,TWARAY(1)
      D=DRTAP/DRGATE
      L=1
      DO 30 K=1,NARAY
      P=(K-1)/FLOAT(NARAY-1)
      DO 10 J=1,4
      X(J)=CHI(D*(P+2-J))
   10 CONTINUE
      DO 20 I=1,4
      DO 20 J=1,4
      A(I,J)=CHI(D*(I-J))
   20 CONTINUE
      CALL SIMQ(A,X,4,IERR)
      IF(IERR.GT.0) STOP
      CALL XMIT(4,X,TWARAY(L))
      L=L+4
   30 CONTINUE
      RETURN
      END
```

```
      FUNCTION CHI(P)
C
C RANGE GATE RESPONSE.  THE ARGUMENT P IS THE RANGE MISMATCH NORMALIZED
C TO THE RECEIVER GATE SPACING.  INTERPOLATION IS USED ON THE SAMPLES
C STORED IN THE A-ARRAY, WHERE THE SPACING IS 0.1 UNIT.
C
C THE RESIDUAL ERROR IN THE INTERPOLATION IS LESS THAN .0003
C
C P MUST BE LESS THAN 1.5 IN MAGNITUDE.
C
C THE SAMPLES ARE OF THE RESPONSE DERIVED IN MRI REPORT 149-4.
C
      DIMENSION A(18)
      DATA A/1.00000, .98104, .92193, .81903, .67431, .50112, .32385,
     1      .17071, .06308, .00731,-.00651, .00182, .01262, .01458,
     2      .00713,-.00313,-.00898,-.00762 /
      H=10.*ABS(P)
      IF(H.GT.15.) STOP 55
      I=H
      H=H-I
      IP1=I+1
      IP2=I+2
      IP3=I+3
      IF(I.LE.0) I=2
      CHI=-.166667*H*(H-1.)*(H-2.)*A(I)+.5*(H**2-1.)*(H-2.)*A(IP1)
     1   -.5*H*(H+1.)*(H-2.)*A(IP2)+.166667*H*(H**2-1.)*A(IP3)
      RETURN
      END
```

```
      SUBROUTINE SIMQ(A,B,N,IERR)
C
C SOLVES SET OF N SIMULTANEOUS EQUATIONS.....
C
C                  A * X = B          SUM (A(I,J)*X(J)) = B(I)
C
C WHERE ARRAY A IS 2-DIMENSIONAL.  ARRAY X IS RETURNED IN ARRAY B, AND
C ARRAY A IS DESTROYED.  COMPUTATION IS VALID IF IERR=0
C
      DIMENSION A(1),B(1)
      IERR = 0
      IF (N.GT.0)   GO TO 10
      IERR = 1
      RETURN
C
C          FORWARD SOLUTION
C
   10 TOL = 0.0
      KS = 0
      JJ = -N
      DO 65 J = 1,N
      JY = J + 1
      JJ = JJ + N + 1
      BIGA = 0.
      IT = JJ - J
      DO 30 I = J,N
C
C          SEARCH FOR MAXIMUM COEFFICIENT IN COLUMN
C
      IJ = IT + I
      IF (ABS(BIGA)-ABS(A(IJ)))   20, 30, 30
   20 BIGA = A(IJ)
      IMAX = I
   30 CONTINUE
C
C          TEST FOR PIVOT LESS THAN TOLERANCE (SINGULAR MATRIX)
C
      IF (ABS(BIGA)-TOL)   35, 35, 40
   35 IERR = 2
      RETURN
C
C          INTERCHANGE ROWS IF NECESSARY
C
   40 I1 = J + N*(J-2)
      IT = IMAX - J
      DO 50 K = J,N
      I1 = I1 + N
      I2 = I1 + IT
      SAVE = A(I1)
      A(I1) = A(I2)
```

```
      A(I2) = SAVE
C
C            DIVIDE EQUATION BY LEADING COEFFICIENT
C
   50 A(I1) = A(I1)/BIGA
      SAVE = B(IMAX)
      B(IMAX) = B(J)
      B(J) = SAVE/BIGA
C
C            ELIMINATE NEXT VARIABLE
C
      IF (J-N)  55, 70, 55
   55 IQS = N*(J-1)
      DO 65 IX = JY,N
      IXJ = IQS + IX
      IT = J - IX
      DO 60 JX = JY,N
      IXJX = N*(JX-1) + IX
      JJX = IXJX + IT
   60 A(IXJX) = A(IXJX) - (A(IXJ)*A(JJX))
   65 B(IX) = B(IX) - (B(J)*A(IXJ))
C
C            BA SOLUTION
C
   70 NY = N - 1
      IT = N*N
      DO 80 J = 1,NY
      IA = IT - J
      IB = N - J
      IC = N
      DO 80 K = 1,J
      B(IB) = B(IB) - A(IA)*B(IC)
      IA = IA - N
   80 IC = IC - 1
      RETURN
      END
```

```
      SUBROUTINE XMIT(N,A,B)
C
C IN THIS SUBROUTINE WE EITHER TRANSMIT ARRAY A TO ARRAY B (IF N.GT.0)
C OR WE TRANSMIT THE CONSTANT A TO ARRAY B (IF N.LT.0).  IN EITHER CASE
C THE ARRAY LENGTH IS IABS(N).
C
C THIS SUBROUTINE SHOULD BE WRITTEN IN ASSEMBLY LANGUAGE
C
      DIMENSION A(1),B(1)
      IF(N) 10,20,25
   10 NN=-N
      AA=A(1)
      DO 15 K=1,NN
      B(K)=AA
   15 CONTINUE
   20 RETURN
   25 DO 30 K=1,N
      B(K)=A(K)
   30 CONTINUE
      RETURN
      END
```

```
      SUBROUTINE SINCOS(ARG,S,C)
C
C THIS SUBROUTINE SHOULD BE WRITTEN IN ASSEMBLY LANGUAGE, USING THE
C TABLE-LOOKUP METHOD DESCRIBED BY MITCHELL (RADAR SIGNAL SIMULATION).
C
      S=SIN(ARG)
      C=COS(ARG)
      RETURN
      END
```

```
      SUBROUTINE ETGD1(DTIME)
C
C GLINT AND DOPPLER MODULATION FOR N-POINT SCATTER MODEL
C
C NO RANGE EXTENSION
C
C SUBROUTINE REPLACES ETGDM
C
C ON INPUT.....

C               DTIME  = TIME SINCE LAST UPDATE IN TARGEO
C
C       /T5/    XL     = WAVELENGTH
C               PTGDSQ = PRODUCT OF TRANSMIT POWER, GAIN, AND SQUARE OF
C                        RFSS CHAMBER LENGTH
C
C       /T7/    NS     = NUMBER OF SCATTERERS VISIBLE
C               AMP(J) = AMPLITUDE OF J-TH SCATTERER
C               DA(J)  = INCREMENTAL A-VECTOR OF J-TH SCATTERER
C               DB(J)  = INCREMENTAL B-VECTOR OF J-TH SCATTERER
C               DC(J)  = INCREMENTAL C-VECTOR OF J-TH SCATTERER
C               DAD(J) = INCREMENTAL A-VECTOR RATE OF J-TH SCATTERER
C
C ON OUTPUT.....
C
C       /T8/    PEFF   = EFFECTIVE RADIATED POWER AT RFSS ARRAY
C
C       /T9/    VR,VI       = DOPPLER MODULATION SIGNAL
C               DR,DAZ,DEL = RANGE,AZIMUTH, AND ELEVATION GLINT OFFSETS
C
      COMMON /T5/ NTAP,DRTAP,DRGATE,XL,PTGDSQ
      COMMON /T7/ NS,RO,R1,ROD,AMP(20),DA(20),DB(20),DC(20),DAD(20)
      COMMON /T8/ PEFF
      COMMON /T9/ VR,VI,DR,DAZ,DEL
      DATA FOURPI/12.5663706/
C
C ZERO ACCUMULATORS
C
      VR=0.
      VI=0.
      VAR=0.
      VAI=0.
      VBR=0.
      VBI=0.
      VCR=0.
      VCI=0.
C
C LOOP OVER NS SCATTERERS
C
      DO 40 J=1,NS
```

```
      CALL SINCOS(FOURPI*(DA(J)+DAD(J)*DTIME)/XL,S,C)
      C=C*AMP(J)
      S=S*AMP(J)
      VR =VR +C
      VI =VI +S
      VAR=VAR+C*DA(J)
      VAI=VAI+S*DA(J)
      VBR=VBR+C*DB(J)
      VBI=VBI+S*DB(J)
      VCR=VCR+C*DC(J)
      VCI=VCI+S*DC(J)
   40 CONTINUE

      POW=VR**2+VI**2
      AMPL=SQRT(POW)
C
C COMPUTE GLINT OFFSETS
C
      DR =-(VAR*VR+VAI*VI)/POW
      DAZ=-(VBR*VR+VBI*VI)/(RO*POW)
      DEL=-(VCR*VR+VCI*VI)/(RO*POW)
C
C COMPUTE EFFECTIVE RF POWER
C
      PEFF=POW*PTGDSQ/(FOURPI*RO**4)
C
C NORMALIZE
C
      VR=VR/AMPL
      VI=VI/AMPL

      RETURN
      END
```

```
      SUBROUTINE DATAIN
C
C READS TARGET SCATTERING DATA SUPPLIED BY M.MUMFORD (SEE SCTAMP).
C
      DIMENSION IA(1),AA(4),XX(4),YY(4),ZZ(4)
      COMMON /DP/ P(100),IP(100)
      COMMON /DQ/ Q(918)
      COMMON /T4/ NSCAT
      DATA LR,LW/5,6/
      NSCAT=10
      M=1
      DO 20 I=1,NSCAT
      PRINT 99,I
      L=10*(I-1)
   10 L=L+1
      READ  (LR,100) IA,P(L),AA,XX,YY,ZZ
      WRITE (LW,100) IA,P(L),AA,XX,YY,ZZ
      IP(L)=M
      IA=IA-2
      CALL XMIT(17,IA,Q(M))
      M=M+17
      IF(P(L).LT.180.) GO TO 10
   20 CONTINUE
      RETURN
   99 FORMAT(/29H TARGET DATA FOR SCATTERER NOI3//)
  100 FORMAT(1XI1,12XF8.3,4E14.8/(22X4E14.8))
      END
```

```
      FUNCTION SCTAMP(K,ANGL)
C
C IN THIS SUBROUTINE WE COMPUTE THE AMPLITUDE (SQRT(RCS)) OF THE K-TH
C SCATTERER AS VIEWED FROM THE TARGET ASPECT.....
C
C     ANGL = ANGLE FROM ROLL AXIS MEASURED FROM NOSE (RAD)
C
C IN ADDITION IN COMMON /T4/.....
C
C       ST = BIAS THAT IS ADDED TO ANGL (RAD)
C
C THIS SUBROUTINE ACCESSES TARGET DATA SUPPLIED BY MIKE MUMFORD AT NWC/
C CHINA LAKE IN THE FORMAT DEFINED BY A COMPUTER PROGRAM WRITTEN 5/11/78
C BY E.HUTTON X3219.
C
      DIMENSION IA(1),AA(4),XX(4),YY(4),ZZ(4)
      COMMON /T4/ NSCAT,ST,AMPMIN,X(20),Y(20),Z(20)
      COMMON /DP/ P(100),IP(100)
      COMMON /DQ/ Q(918)

      ANG=ABS(ANGL+ST)*57.2957795
      IF(ANG.GT.180.) ANG=180.
      I1=10*(K-1)+1
      I2=I1+9
      DO 20 I=I1,I2
      IF(ANG.LT.P(I)) GO TO 25
   20 CONTINUE
   25 M=IP(I)
      CALL XMIT(17,Q(M),IA)
      IF(IA) 30,31,32
   30 SCTAMP=AA(1)+ANG*(AA(2)+ANG*(AA(3)+ANG*AA(4)))
      GO TO 35
   31 SCTAMP=EXP(AA(1)+ANG*AA(2))
      GO TO 35
   32 SCTAMP=EXP(AA(1)+ANG*AA(2))-EXP(AA(3)+ANG*AA(4))
   35 SCTAMP=.09004*SCTAMP
      IF(SCTAMP.LT.AMPMIN) RETURN
      X(K)=XX(1)+ANG*(XX(2)+ANG*(XX(3)+ANG*XX(4)))
      Y(K)=YY(1)+ANG*(YY(2)+ANG*(YY(3)+ANG*YY(4)))
      Z(K)=ZZ(1)+ANG*(ZZ(2)+ANG*(ZZ(3)+ANG*ZZ(4)))
      Y(K)=-Y(K)
      Z(K)=-Z(K)
      RETURN
      END
```

DAT

ILM